Bioorganic Chemistry 92 (2019) 103255

Contents lists available at ScienceDirect

Bioorganic Chemistry

journal homepage: www.elsevier.com/locate/bioorg

Design, synthesis, and biological activity of Plastoquinone analogs as a new class of anticancer agents

Nilüfer Bayrak[a], Hatice Yıldırım[a], Mahmut Yıldız[b], Mohamed O. Radwan[c,d,e], Masami Otsuka[c,d], Mikako Fujita[f,*], Amaç Fatih Tuyun[g,*], Halil I. Ciftci[c,d,*]

[a] Chemistry Department, Engineering Faculty, Istanbul University-Cerrahpasa, Avcilar, 34320 Istanbul, Turkey
[b] Chemistry Department, Gebze Technical University, Gebze 41400, Kocaeli, Turkey
[c] Department of Drug Discovery, Science Farm Ltd., Kumamoto 860-0802, Japan
[d] Department of Bioorganic Medicinal Chemistry, School of Pharmacy, Kumamoto University, Kumamoto 862-0973, Japan
[e] Chemistry of Natural Compounds Department, Pharmaceutical and Drug Industries Research Division, National Research Centre, Dokki 12622, Cairo, Egypt
[f] Research Institute for Drug Discovery, School of Pharmacy, Kumamoto University, Kumamoto 862-0973, Japan
[g] Engineering Sciences Department, Engineering Faculty, Istanbul University-Cerrahpasa, Avcilar, 34320 Istanbul, Turkey

ARTICLE INFO

Keywords:
Plastoquinone
Aminoquinone
Apoptosis
Bcr-Abl
DNA-cleavage
Structure-activity relationship (SAR)

ABSTRACT

In this paper, based on Plastoquinone (PQ) analogs possessing substituted aniline containing alkoxy group(s), new 2,3-dimethyl-5-amino-1,4-benzoquinones (**PQ1-15**) were designed and synthesized in either two steps or one-pot reaction. Specifically, the substituted amino moiety containing mono or poly alkoxy group(s) with various positions and groups were mainly explored to understand the structure-activity relationships for the cytotoxic activity against three human cancer cell lines (K562, Jurkat, and MT-2) and human peripheral blood mononuclear cells (PBMC). **PQ2** was found to be most effective anticancer compound on K562 and Jurkat cell lines with IC_{50} values of 6.40 ± 1.73 μM and 7.72 ± 1.49 μM, respectively. Interestingly, the compound was non-cytotoxic to normal PBMC and also MT-2 cancer cells. **PQ2** which showed significant selectivity in MTT assay was chosen for apoptotic/necrotic evaluation and results exhibited that it induced apoptosis in K562 cell line after 6 h of treatment. **PQ2** showed anti-Abelson kinase 1 (Abl1) activity with different inhibitory profile than Imatinib in the panel of eight kinases. The binding mode of **PQ2** into Abl ATP binding pocket was predicted *in silico* showing the formation of some key interactions. In addition, **PQ2** induced Bcr-Abl1 mediated ERK pathway in human chronic myelogenous leukemia (CML) cells. Furthermore, DNA-cleaving capability of **PQ2** was clearly enhanced by iron (II) complex system. Afterward, a further *in silico* ADMET prediction revealed that **PQ2** possesses desirable drug-like properties and favorable safety profile. These results indicated that **PQ2** has multiple mechanism of action and two of them are anti-Bcr-Abl1 and DNA-cleaving activity. This study suggests that Plastoquinone analogs could be potential candidates for multi-target anticancer therapy.

1. Introduction

Cancer is the most common human genetic disease that could affect all people in the world regardless of race, age, or socioeconomic status. Cancer starts in cells that are the smallest part of body and to know the normal cell cycle processes and how a breakdown in the regulation of this cycle occurs provides an understanding the mechanisms of cancer. According to the report of the World Health Organization (WHO), nearly 1 in 6 global deaths (8,8 million people) in 2015 is due to cancer and this rates could further increase by 50% (15 million people) in the year 2020 [1,2]. Around 360,000 deaths in 1,192,000 total deaths occurred from cancer in Japan in other words this illness was the killer of approximately 1 in every 3 people in 2014. The number in Turkey was reported as 90,000 in 422,000 total deaths in the same year revealed that 1 in every 5 people have been killed by this risky disease [3]. In all types of cancer, uncontrolled growth of abnormal cells that refers cancer, malignant, or tumor cells begin to divide without stopping and invade surrounding tissues [2]. Not only genetic changes can cause cancer but it also can arise throughout the lifespan as a result of failures in cell division or due to DNA damage caused by certain environmental

* Corresponding authors at: Research Institute for Drug Discovery, School of Pharmacy, Kumamoto University, Kumamoto 862-0973, Japan (M. Fujita), Engineering Sciences Department, Engineering Faculty, Istanbul University-Cerrahpasa, Avcilar, 34320 Istanbul, Turkey (A.F. Tuyun), and Department of Bioorganic Medicinal Chemistry, School of Pharmacy, Kumamoto University, Kumamoto 862-0973, Japan (H.I. Ciftci).
E-mail addresses: mfujita@kumammot-u.ac.jp (M. Fujita), aftuyun@istanbul.edu.tr (A.F. Tuyun), hiciftci@kumamoto-u.ac.jp (H.I. Ciftci).

https://doi.org/10.1016/j.bioorg.2019.103255
Received 13 February 2019; Received in revised form 30 July 2019; Accepted 4 September 2019
Available online 07 September 2019
0045-2068/

exposures such as tobacco and alcohol use, infections, and environmental pollution [4].

From the first time ever a description of cancer was seen in an Egyptian papyrus in 1600 BCE to the nineteenth century, it was thought as an inevitably fatal illness [5]. The beginning of nineteenth century was a period of surgical treatment which is the most effective in the treatment of localized primary tumors [6], and subject to radiation therapy (by X-rays and gamma rays) used to control the disease after 1960 [5]. After finding out surgery and radiation, even a combination of both, wasn't succeeding adequately in management of the metastatic cancer due to the fact that therapy does not reach all parts of the body. Next steps in the discovery of a cure for cancer have been focusing on chemotherapy drugs, biological molecules, and immune mediated therapies [5]. One of the most common treatments for cancer is chemotherapy that is the use of drugs to kill cancer cells or slow their growth [7]. Chemotherapy drugs can be given in a variety of different ways including orally or by injection. They are delivered *via* the blood circulatory system to all parts of the body so they have been effective in cancer that has spread [8,9]. There has been continuing a struggle between cancer and scientists who strive to overcome the possibly fatal disease by using a combination of treatments, such as surgery with chemotherapy and radiation therapy. Unfortunately, in addition to adverse side effects of chemotherapy such as anaemia, diarrhoea, hair loss, and weakening of the immune system, chemotherapeutic drugs resistance may occur sooner or later in cancer cells [6]. Toxicity with conventional chemotherapeutic drugs and damage to normal cells from treatment have led to the development of targeted therapies. In recent years, with the specific aim of reducing side effects and increasing the effectiveness of cancer treatment, tyrosine kinase inhibitors (TKIs), monoclonal antibodies, bortezomib, and other drugs such as thalidomide have become increasingly adept at targeted therapies [10]. Among these, TKIs have been widely used in the treatment of many cancers, especially in chronic myeloid leukemia (CML) since TKIs are more effective than other treatments such as chemotherapy and radiotherapy by focusing on molecular and cellular changes and less harm to normal cells [11]. TKIs inhibit the phosphorylation of protein catalyzed by tyrosine kinases, stop cell cycle, and provide apoptosis of the tumor cell [12]. The TKIs especially used in CML approved by the US Food and Drug Administration (FDA) are Bosutinib, Dasatinib, Imatinib, Nilotinib, and Ponatinib [13]. Imatinib is the first Bcr-Abl TKI as a specific inhibitor for the treatment of CML, subsequently, other drugs have been used [14]. While Imatinib can be initially effective on early stage CML, but it is less effective in advanced stage CML due to resistance development [15,16]. The most important cause of progressive resistance is the mutations in the Bcr-Abl kinase region. Nowadays, new generation small molecules have been developed by many researches to increase the therapeutic efficacy of Imatinib and overcome its resistance [17,18].

Currently, the exploration for the new lead molecules for cancer treatment in natural products is the best way of modern pharmaceutical research since they are generally thought to be less toxic and side effects. A lot of major novel drugs have been obtained from natural products as a source of bioactive compounds for thousands of years in the world [19–21]. There are clearly two major points that prove the importance of the natural products. First, they provide us the new drugs and/or lead compounds that would be inaccessible by "medicinal chemistry" approaches. Henkel et al. previously mentioned that "40% of the natural products are not represented by synthetic compounds" in a data set containing more than 200,000 chemical compounds [22]. Second, they provide us with important templates for the design of new drugs in the future. Sometimes, even if there is a novel pharmacophore in an isolated compound, the compound may not be a lead compound for various reasons. After a new pharmacophore has been discovered, the medicinal and/or organic chemists try to improve it by modifying the moiety of the isolated compound. Some important bioactive compounds, especially methyl substituted 1,4-benzoquinones, are shown in Fig. 1 including Thymoquinone (TQ) [23,24], Plastoquinones (PQ), and Mitomycin C [25,26]. One of the representative studies engineered versatile TQ analogs and they were tested for their anticancer activity against some pancreatic cancer cell lines. Among these analogs, three analogs were found to have a great anticancer activity [27]. In 2018, Johnson-Ajinwo et al. reported the novel TQ analogs with the evaluation of their antiproliferative activity against ovarian cancer cell lines and human malaria parasite [28]. The discovery of the PQ (Fig. 1) in 1946 by Barr for electron transfer in photosynthesis was the beginning of an inevitable role in plant growth and development [29].

During the last few years, our group is dedicated to develop new bioactive substances with potential applications as pharmaceuticals especially anticancer and/or antimicrobial agents based on aminoquinones and/or thioquinones [30,31]. Attention and applications into aminoquinones have greatly increased in recent years [32–37]. Aminoquinones are considered to be not only versatile synthetic synthons [37–41] but also pharmacologically active substances displaying a wide range spectrum such as antibacterial [42–44], antifungal [45,46], anticancer [47,48], antimalarial [49], antiviral [50], and antitubercular activity [51]. In this article, to explore the possibility of the aminoquinone compounds as a pivotally structure in TKIs, we, therefore, designed, synthesized potent aminobenzoquinones named PQ analogs with lower IC_{50}, and studied their anti-Bcr-Abl and DNA-cleavage activities using cellular and *in vitro* assays. PQ, TQ, and Mitomycin C (Fig. 1) were used as lead molecules for the design.

2. Results and discussion

2.1. Design and chemical synthesis

Quinones' electrophilic character enables them to undergo nucleophilic addition with electron-rich nucleophilic species such as amines, thiols, and alcohols. Medicinal and/or organic chemists are often interested in synthesis of novel analogs of the discovered pharmacophore moiety in isolated natural molecules with lower IC_{50} in order to develop new therapeutic agents for the treatment of diseases [52–54]. In addition to obtain new analogs with different side chains of PQ [55], cationic benzoquinones were synthesized with positively charged phosphonium or rhodamine moiety attached to PQ as mitochondria-targeted antioxidants [56].

Building a library of PQ analogs (**PQ1-15**) started with the design based on PQ, TQ, and Mitomycin C. Scheme 1, initially, illustrates the retrosynthetic analyses of the PQ analogs that could be easily prepared from the commercially available 2,3-dimethylhydroquinone (**1**) in one or two steps. Firstly, oxidation of commercially available 2,3-dimethylhydroquinone (**1**) by oxidant ($KBrO_3$ [57] or MnO_2 [58]) resulted in the production of 2,3-dimethyl-1,4-benzoquinone (**2**) in 98% or 86% yield, respectively. Then, last step of synthesis accomplished by the reaction of 2,3-dimethyl-1,4-benzoquinone (**2**) with the corresponding substituted anilines in ethanol at reflux (Scheme 2) according to reported procedure, but in the absence of $CeCl_3$ [59]. To our delight, it is worth mentioning that a simple one-pot reaction is also performed starting from the commercially available 2,3-dimethylhydroquinone (**1**) with the corresponding substituted anilines in the presence of oxidant ($NaIO_3$) (Scheme 2) according to reported procedure [60]. Among these, **PQ2** [61] and **PQ8** [62] are known molecules reported in the literature before, while the other PQ analogs are novel molecules.

The chemical structures of the PQ analogs (**PQ1-15**, Table 1) were determined on the basis of their spectral properties by FTIR, ^{1}H NMR, ^{13}C NMR, and MS. The FTIR spectra of PQ analogs revealed the characteristic absorption band of carbonyl groups (> C═O) at around 1636–1666 cm^{-1} and N−H group at around 3223–3349 cm^{-1}. ^{1}H NMR spectra displayed a broad singlet corresponding to one NH proton in the range of 7.08–7.90 ppm. The signals of the protons on methoxy groups were observed a singlet in the range of 3.71–3.83 ppm as expected. Further evidence in support of a formation of PQ analogs came by

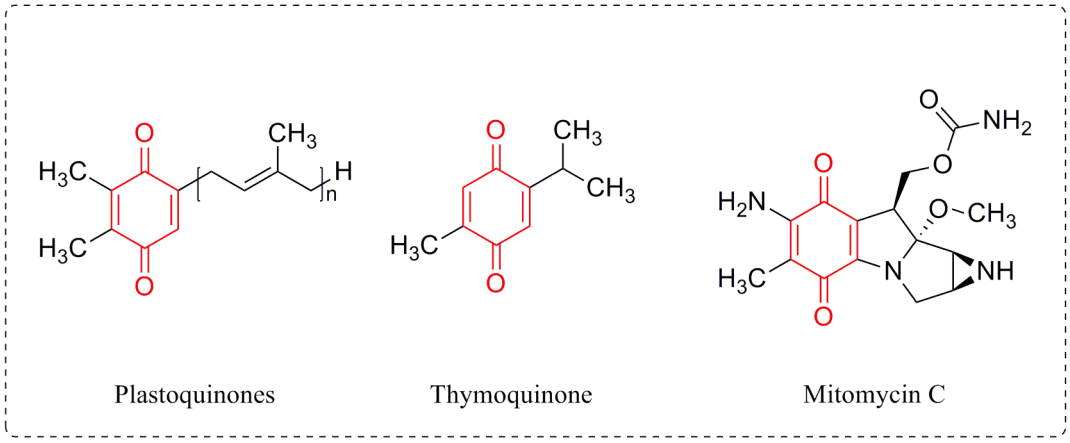

Fig. 1. Bioactive compounds containing quinone moiety in natural products.

recording their ^{13}C NMR spectra which showed the two characteristic signals of quinone moiety at around 183 and 187 ppm due to the two carbonyl groups (> C=O). In ^{13}C NMR spectra, two carbon atoms in the methyl groups of quinone moiety (C-2 and C-3) and carbon atoms of methoxy groups were displayed at around 12 and 15 ppm and in the range of 55–61 ppm, respectively. Chemical shifts of other protons and related carbons were reported in experimental section with all details. Additionally, the structures of the **PQ1** (1891326), **PQ4** (1891328), **PQ11** (1891330), and **PQ14** (1891331) were further confirmed by the single crystal diffraction (Fig. 2) (For details, please see the Supplementary file).

2.2. Biological evaluation

To assess the cytotoxicity, PQ analogs (**PQ1-15**) were examined for their anticancer activities against three cancer cell lines by MTT assay including K562 (chronic myelogenous leukemia), Jurkat, MT-2 (other leukemias), and peripheral blood mononuclear cells (PBMC) as summarized in Tables 1 and 2 and Fig. 3. As shown in Table 1, PQ analogs were designed to explore the effect of methoxy group(s) and positions, and, additionally, the methoxy group was also replaced with ethoxy and butoxy group in the substituted amino moiety to investigate the effect of the alkyl chain on cytotoxicity. In the case of MT-2 cell, the compound **PQ10** with dimethoxy group showed the anticancer activity with the IC_{50} value of 35.79 μM. Some of the tested compounds (**PQ3**, **PQ6**, **PQ9-12**, and **PQ14-15**) were found to possess the IC_{50} values lower than 30 μM against Jurkat cell. The analogs (**PQ2** and **PQ5**) containing alkoxy group (methoxy and ethoxy, respectively) at the 3-position in the aryl amino moiety showed better anticancer activity than the control drug Imatinib against Jurkat cell (Fig. 3b). Among the PQ analogs, **PQ2**, **PQ3**, and **PQ10** were shown to be the most potent compounds against K562 cell line with the IC_{50} value of 6.40 μM, 9.66 μM, and 8.91 μM respectively (Fig. 3a). Other analogs except that the analogs (**PQ1**, **PQ4**, **PQ7**, and **PQ11-13**) exerted comparable activities with IC_{50} less than 30 μM against K562 cell. Additionally, some analogs (**PQ1**, **PQ4**, **PQ7**, and **PQ13**) showed no significant activity against the all three cell lines.

Moreover, the cytotoxicity of selected PQ analogs (**PQ2**, **PQ3**, and **PQ10**) on PBMC was also tested as shown in Fig. 3c. As the selective index (SI) is calculated as the ratio of cytotoxicity of the IC_{50} between the PBMC and K562 cells, the greater the SI value, the more selective for cancer cells. The results revealed that the most active analog **PQ2** against K562 cell had the highest SI with the value of over 46.88 (Table 2).

The structure–activity relationships (SAR) were investigated by modification of various positions (mono- or polysubstituted) with different alkoxy group(s) in the substituted amino moiety since the same substituent at different positions may change the activity. Taken as whole, these results indicate some important points. For the analogs containing monosubstituted alkoxy group in the amino moiety, the

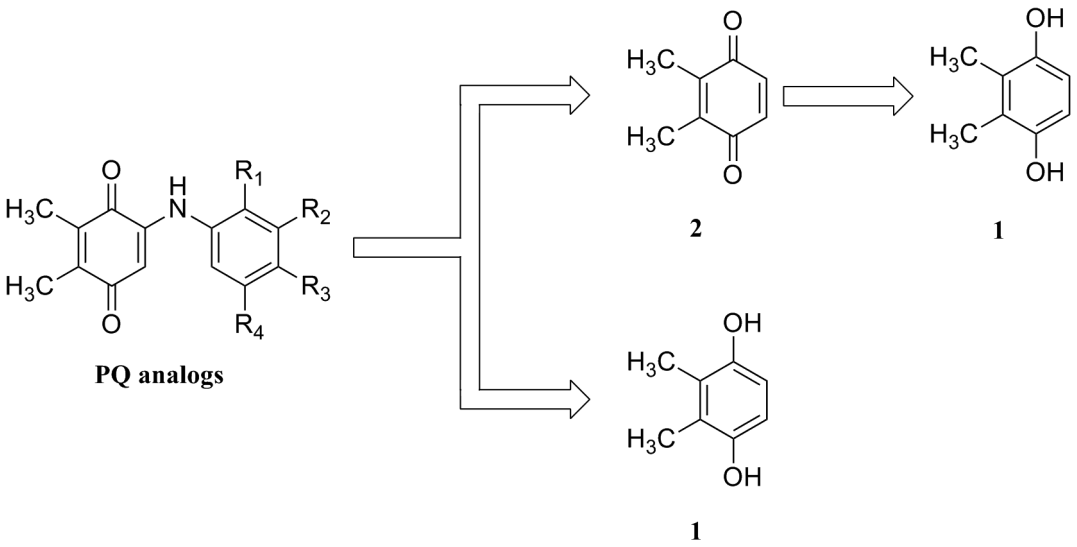

Scheme 1. Retrosynthetic analyses of PQ analogs.

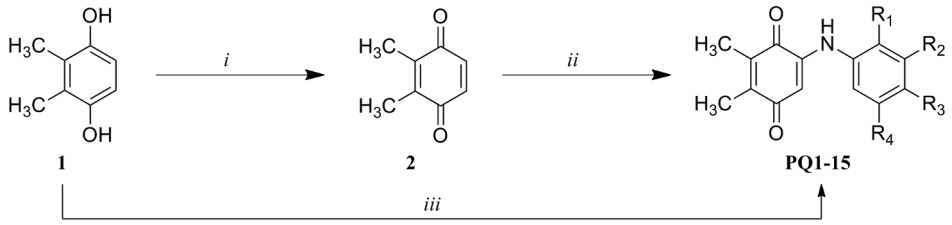

Scheme 2. Preparation of PQ analogs (**PQ1-15**). Reagents and conditions: (i) $KBrO_3$, H_2SO_4/H_2O, 10 min, 80 °C; (ii) Substituted anilines, EtOH, reflux, 4–12 h; (iii) Substituted anilines, $NaIO_3$, H_2O, rt, 10–24 h.

alkoxy group at the 2-position did not show the good cytotoxic activities. The analogs with alkoxy group at the 4-position had relatively higher potency but the monosubstituted alkoxy at the 3-position led to a considerable increase in potency against K562 and Jurkat cell lines. Among the analogs containing polysubstituted alkoxy group in the amino moiety, the compounds containing the dimethoxy in 3,5-positions (**PQ11**) led to a large reduction in activity compared to compounds containing the dialkoxy in 2,3-positions (**PQ10** and **PQ14**). However, we could say that the compounds having specifically alkoxy group(s) at the 3-position were found to be more potent against K562 and Jurkat cell lines, but the addition of the methoxy group led to decrease the activities. With the elongation of the alkyl tail in the alkoxy group, the cytotoxic activities decreased in the obtained analogs (i.e., **PQ2** vs **PQ5**, **PQ6** vs **PQ7**, and **PQ9** vs **PQ12**).

MTT results showed that **PQ2** was the most active and selective anticancer compound in this series, and was chosen to investigate its apoptotic and necrotic activity in K562 cell line. Thus, the annexin V/ethidium homodimer III and Hoechst 33,342 staining method was carried out with K562 cell line-treated **PQ2** at IC_{50} concentration and then observed by a fluorescence microscope (Fig. 4). In the control experiment, all cells were stained with blue (healthy cells) at 6 h after treatment of DMSO (Fig. 4a). On the contrary, K562 cells treated-**PQ2** and Imatinib were stained mostly with healthy cells (blue), then with apoptotic cells (green), late apoptotic or necrotic cells (both green and red), and necrotic cells (red) (Fig. 4a), suggesting that **PQ2** and Imatinib induced apoptosis mainly in earlier time. The results indicated that **PQ2** has 69% apoptotic, 20% late apoptotic/necrotic, and 11% necrotic effects at 6 h as illustrated in Fig. 4b. The response of K562 cells upon 6 h Imatinib treatment was 63% apoptosis, 19% late apoptosis/necrosis, and 18% necrosis (Fig. 4b). The results revealed that **PQ2** induced more cell apoptosis than Imatinib in CML.

In order to explore the inhibition profile of **PQ2** on tyrosine kinase enzymes, a panel of kinases including Abl1, BRK, BTK, CSK, FYN A, LCK, LYN B, and SRC were selected. In this activity-based kinase system, inhibitory effects of **PQ2** were tested using multipoint dose-response experiments. The results are presented in Fig. 5. Among these eight kinases, **PQ2** showed the most potent inhibitory activity against the Abl1 kinase enzyme (IC_{50} = 19.22 ± 3.16 μM). Imatinib was used for comparison and demonstrated stronger inhibition than **PQ2** against Abl1 (IC_{50} = 0.27 ± 0.04 μM). On the other hand, the activity of Imatinib was weaker than that of **PQ2** on BTK and SRC. Kinase inhibitory activity of **PQ2** on selected kinase family revealed the following potency order: Abl1 > SRC > BRK > CSK > BTK with the IC_{50} value of 19.22 ± 3.16 μM, 26.21 ± 2.09 μM 31.54 ± 2.92 μM, 40.76 ± 3.87 μM, and 89.99 ± 6.15 μM, respectively. Furthermore, this compound was found to be inactive against FYN A, LCK, and LYN B. These results pointed out that **PQ2** inhibits multiple kinases in the panel of eight kinases with different kinase inhibitory profile than Imatinib.

Furthermore, we explored the binding mode of **PQ2** into the ATP binding site of Abl kinase to get more insight into its potential interaction pattern. In spite of different stereo-electronic features and molecular weight from Imatinib, **PQ2** could make some key interactions

Table 1
Structure and Cytotoxicity of PQ Analogs (**PQ1-15**) in K562, Jurkat, and MT-2 Cell Lines by MTT Assay.

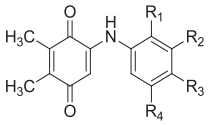

PQ1-15

ID	Substitution Groups				Cell Type (IC_{50}, μM)[a]		
	R_1	R_2	R_3	R_4	K562[b]	Jurkat[b]	MT-2[b]
PQ1	OCH_3	H	H	H	> 30	> 30	> 100
PQ2	H	OCH_3	H	H	6.40 ± 1.73	7.72 ± 1.49	> 100
PQ3	H	H	OCH_3	H	9.66 ± 2.31	22.75 ± 1.93	53.96 ± 3.81
PQ4	OCH_2CH_3	H	H	H	> 30	> 30	> 100
PQ5	H	OCH_2CH_3	H	H	20.43 ± 3.78	8.95 ± 0.87	53.07 ± 4.64
PQ6	H	H	OCH_2CH_3	H	26.6 ± 4.28	22.79 ± 3.91	90.89 ± 5.29
PQ7	H	H	$O(CH_2)_3CH_3$	H	> 30	> 30	> 100
PQ8	OCH_3	H	OCH_3	H	22.28 ± 2.65	> 30	71.63 ± 3.97
PQ9	OCH_3	H	H	OCH_3	29.11 ± 4.07	14.57 ± 1.13	78.77 ± 2.75
PQ10	H	OCH_3	OCH_3	H	8.91 ± 1.26	14.47 ± 1.35	35.79 ± 0.89
PQ11	H	OCH_3	H	OCH_3	> 30	15.07 ± 2.11	> 100
PQ12	OCH_2CH_3	H	H	OCH_2CH_3	> 30	15.95 ± 1.87	> 100
PQ13	H	OCH_2O		H	> 30	> 30	> 100
PQ14	H	OCH_2CH_2O		H	13.88 ± 2.32	21.65 ± 0.91	70.76 ± 4.93
PQ15	H	OCH_3	OCH_3	OCH_3	19.87 ± 3.74	14.39 ± 1.14	51.89 ± 4.41
Imatinib[c]					7.47 ± 2.22	9.49 ± 2.46	22.09 ± 1.76

[a] The reported values represent the mean ± SD for each compound based on three independent experiments.
[b] Cell lines include chronic myelogenous leukemia (K562) and other leukemias (Jurkat and MT-2).
[c] Used as reference.

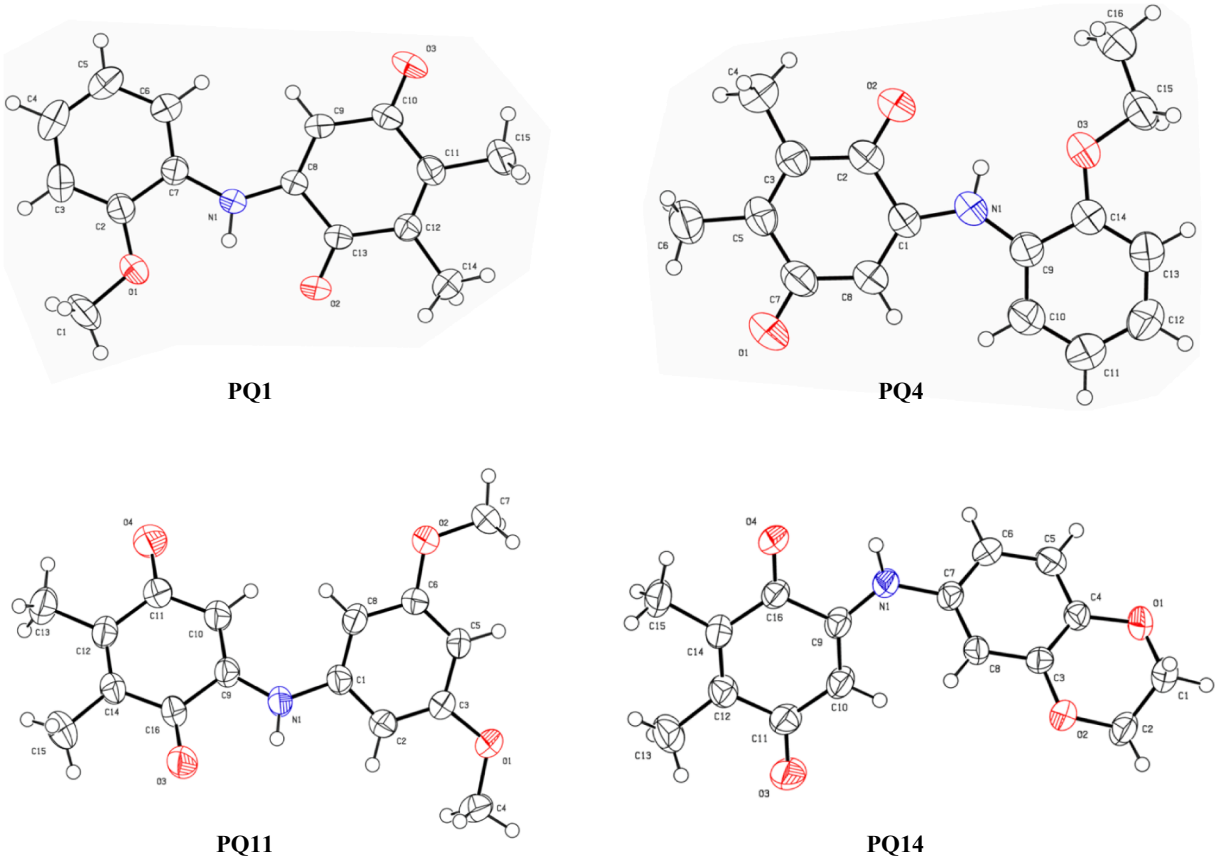

Fig. 2. ORTEP drawings of **PQ1**, **PQ4**, **PQ11**, and **PQ14**.

Table 2
Cytotoxicity of Selected PQ Analogs (**PQ2**, **PQ3**, and **PQ10**) and Selectivity Index (SI).

ID

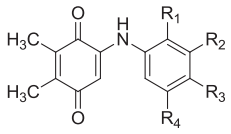

Selected PQ Analogs

	Substitution Groups				Cell Type (IC_{50}, μM)		SI[b]
	R_1	R_2	R_3	R_4	K562[a]	PBMC[a]	
PQ2	H	OCH_3	H	H	6.40 ± 1.73	> 300	> 46.88
PQ3	H	H	OCH_3	H	9.66 ± 2.31	72.68 ± 6.51	7.52
PQ10	H	OCH_3	OCH_3	H	8.91 ± 1.26	69.35 ± 7.12	7.78
Imatinib[c]					7.47 ± 2.22	39.81 ± 4.38	5.33

[a] Cell lines include chronic myelogenous leukemia (K562) and peripheral blood mononuclear cells (PBMC).

[b] The selectivity index (SI) values are calculated as the ratio of the IC_{50} between the peripheral blood mononuclear cells (PBMC) and chronic myelogenous leukemia (K562) cells.

[c] Used as reference.

that conferred it a moderate inhibition as mentioned above. **PQ2** NH forges a key interaction with the gatekeeper Thr315. The C=O of dimethyl benzoquinone forms one more significant hydrogen bond with Met318. Furthermore, the dimethyl benzoquinone makes two CH-π interactions with Leu370 and Tyr253. **PQ2** less affinity, compared to the native ligand Imatinib, may be attributed to missing indispensable bonding with Asp381 and Glu286 (Fig. 6).

As a consequence of the pivotal role of ERK (extracellular signal-regulated kinase) in activation of the mitogen-activated protein kinase (MAPK) signaling cascades for leukemogenesis, K562 cell-treated **PQ2** were evaluated for their inhibitory effects as shown in Fig. 7. **PQ2** showed inhibitory activity on phosphorylation of ERK similar to Imatinib at 20 μM concentration after 6 h of drug treatment. Furthermore, it showed inhibitory activity in a dose dependent manner. It can be concluded that **PQ2** suppresses signaling downstream of tyrosine kinases.

To investigate DNA-cleavage activity of **PQ2**, its capability at IC_{50} concentration were studied using pUC19 DNA with and without the iron (II), H_2O_2, and ascorbic acid complex as shown in Fig. 8. The reaction solution was incubated at 37 °C for 2 h and electrophoresis was performed at 100 V for 30 min. The DNA was stained with ethidium bromide and the gel image was captured by an electronic camera under ultraviolet radiation (UV). The result demonstrated that **PQ2** cleaved the DNA from form I to form II and form III by the activation of the iron complex, suggesting the relationship between the DNA cleavage and the cell death [63].

In order to evaluate the drug-likeness of **PQ2**, we utilized computational calculations of ADMET Predictor 9.0 to predict its risks and physicochemical properties (Fig. 9). **PQ2** toxicity risk (TOX-Risk) value is 2 (acceptable value is up to 3.3). Mutagenic risk (MUT-Risk) value is 2.0, slightly exceeding the standard value 1. Risk related to metabolism by or inhibition of major cytochrome P450s (CYP-Risk) is 0.1 (standard value not exceeds 2.5). Obviously, **PQ2** possesses a potentially appropriate safety profile. **PQ2** exhibited zero violation of Lipinski rule of 5 in terms of (Molecular weight, Log P, tPSA, number of H bond donors and acceptors, and number of rotatable bonds). Concomitantly, absorption risk (Absn-Risk) is 0.0 reflecting a high likelihood of good oral activity. In general, ADMET-Risk value is 2.1 (acceptable value is up to 7.5). In a word, **PQ2** is predicted to have both favorable pharmacokinetic and safety profiles.

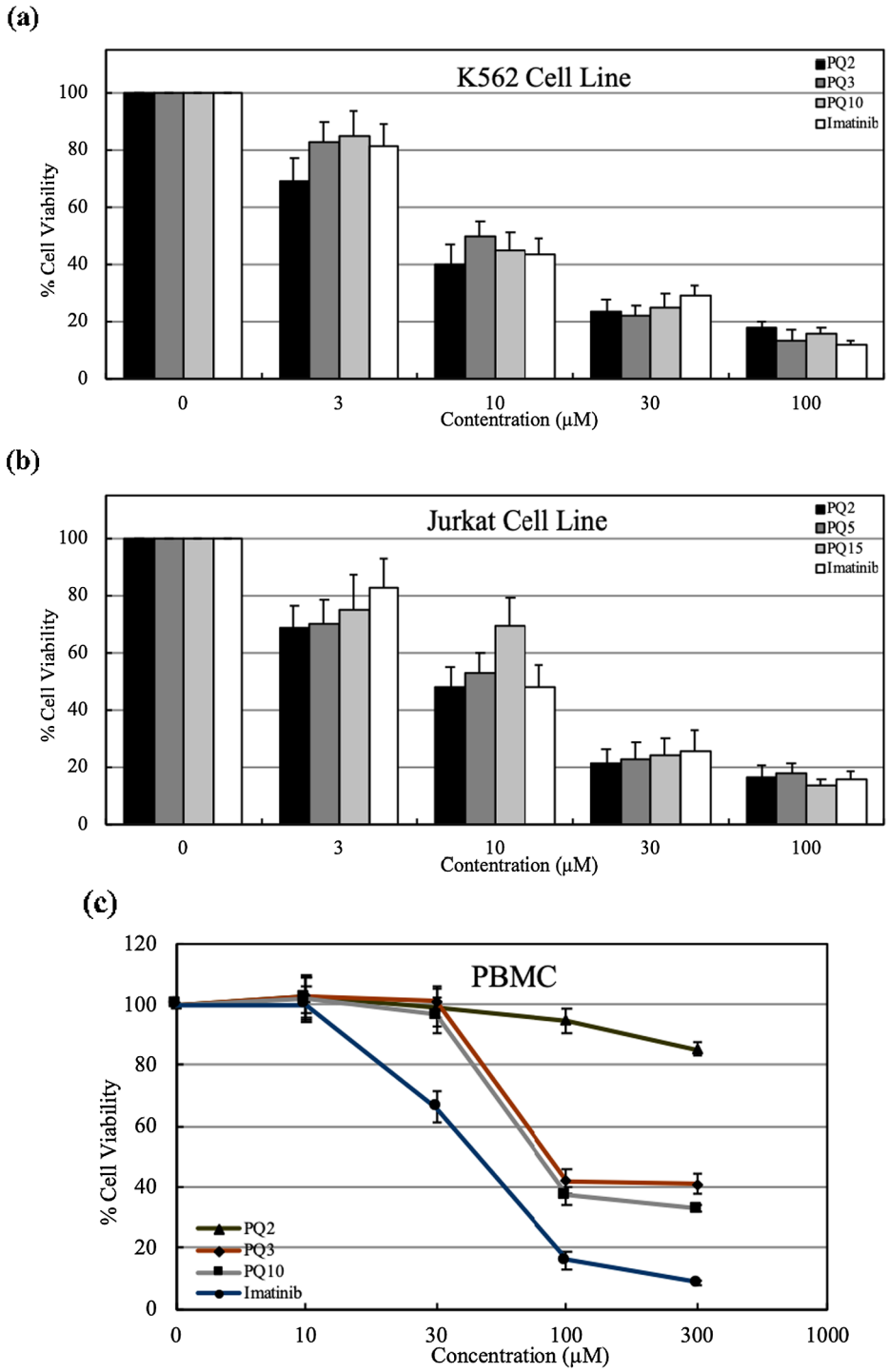

Fig. 3. Anticancer effects of tested compounds and Imatinib on (**a**) K562, (**b**) Jurkat, and (**c**) PBMC cells after 24 h drug treatment.

3. Conclusions

In conclusion, we have synthesized a series of PQ analogs (**PQ1-15**) and examined for their anticancer activities against K562, Jurkat, and MT-2 cell lines. Out of all the compounds evaluated, the analog (**PQ2**) possessing methoxy group at the 3-position in the substituted amino moeity showed the most promising cytotoxic activity against both K562 and Jurkat cell lines, IC_{50} values were 6.40 μM and 7.72 μM, respectively, as well as a low toxicity to PBMC and a high SI compared with the Imatinib. To get more insights into molecular mechanism of PQ analogs, apoptotic/necrotic, DNA cleavage, and kinase profiling were evaluated. The results showed that **PQ2** has considerable apoptotic effect on CML cells when compared with Imatinib and cleaved DNA efficiently. Considering the inhibition profile of **PQ2** on a panel of eight tyrosine kinases, this compound has a different kinase inhibitor profiling than Imatinib. Molecular docking provided the possible binding mode of **PQ2** into the ATP site of Abl1 kinase. Furthermore, *in silico* ADMET prediction highlighted that **PQ2** has desirable drug-like properties and favorable safety profile. This research with the previous studies clearly revealed that action mechanism of **PQ2** (Fig. 10) is considered to be multiple, and two of them are anti-Bcr-Abl1 and DNA-cleaving activity. Further derivatization of Plastoquinone analogs and

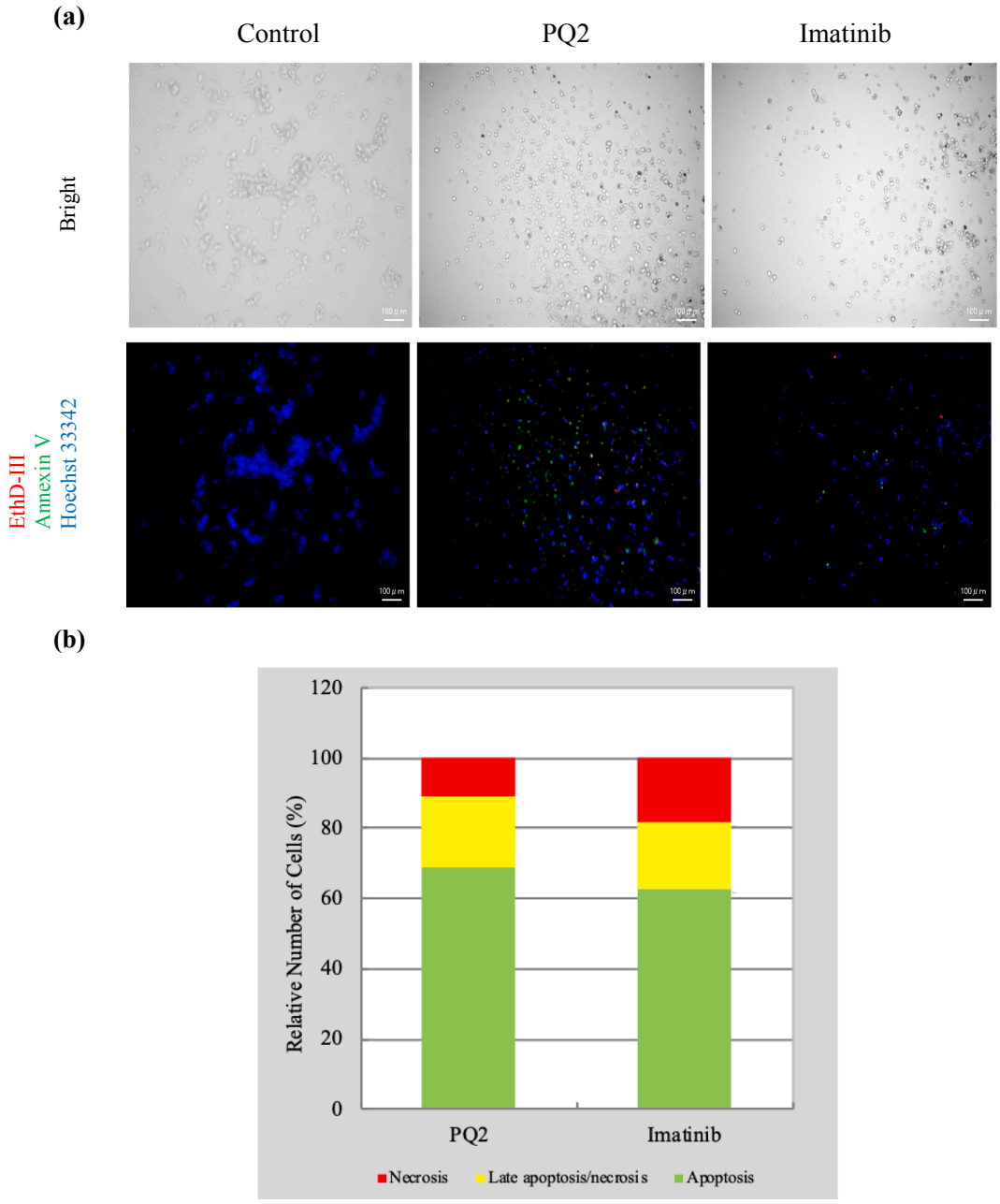

Fig. 4. Alteration in K562 cells at IC_{50} concentrations of **PQ2** and Imatinib (**a**) for 6 h. (**b**) A total of approximate 100 stained cells were selected randomly in each experiment of (A) and were classified into 3 types "apoptosis" (green), "necrosis or late apoptosis" (both green and red), and "necrosis" (red).

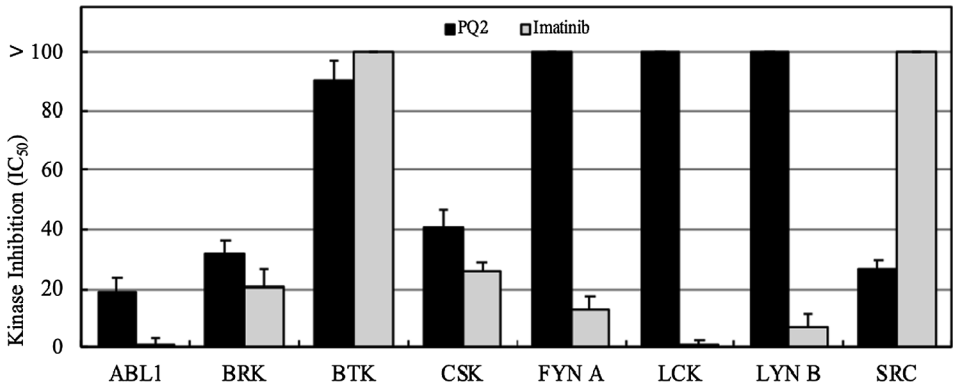

Fig. 5. The inhibition profile of **PQ2** and Imatinib in the panel of eight kinases.

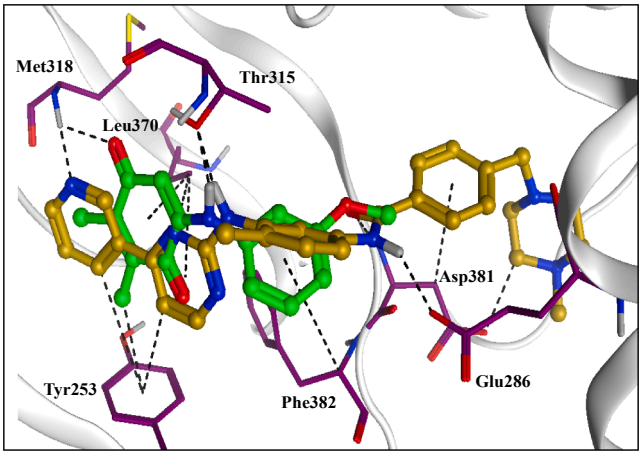

Fig. 6. Binding mode of **PQ2** and Imatinib (green and yellow ball and sticks, respectively) into the ATP binding site of Abl kinase (PDB:1IEP) as calculated by MOE. Key amino acids are depicted in violet sticks. All heteroatoms are colored by element. Ligand-protein interactions are shown as black dash lines.

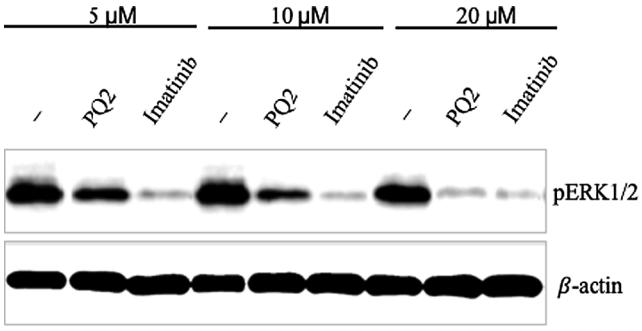

Fig. 7. The effect of **PQ2** and Imatinib on ERK signaling. K562 cells were incubated with tested compounds at 5 μM, 10 μM, and 20 μM for 6 h, and then immunoblot analysis was conducted.

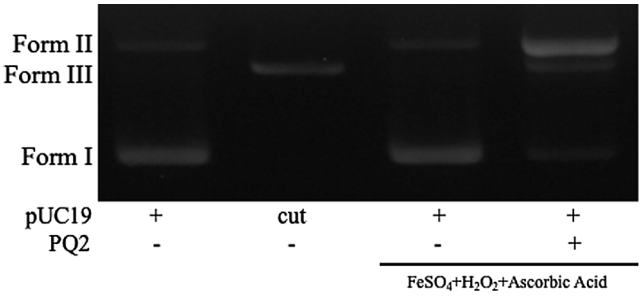

Fig. 8. The DNA-cleaving activity of **PQ2** in the presence and absence of $FeSO_4$, H_2O_2, and ascorbic acid system.

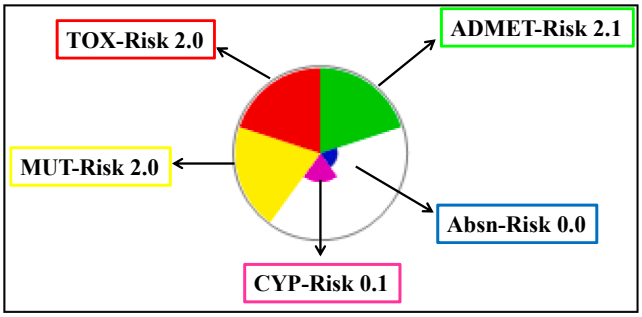

Fig. 9. Star plots depiction for different risk descriptors associated with **PQ2** as calculated by ADMET Predictor 9.0.

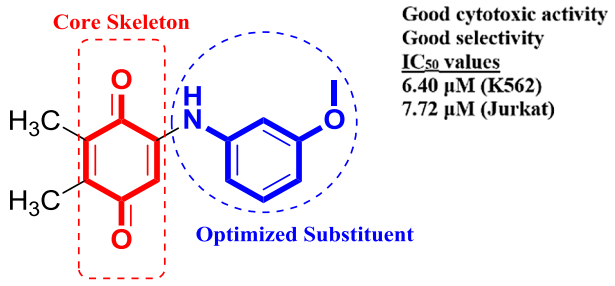

Fig. 10. The optimized active PQ analog (**PQ2**).

their biological investigation for improvement of their anticancer activity are ongoing in our laboratory.

4. Experimental section

4.1. Chemistry

Melting points (mp) were obtained with a Buchi B-540 melting point apparatus and are uncorrected. All reagents were commercially obtained from commercial supplier and used without further purification unless specified otherwise. Thin layer chromatography (TLC) was purchased from Merck KGaA (silica gel 60 F254) based on Merck DC-plates (aluminum based). General compound visualization for TLC was achieved by UV light (254 nm). Column chromatographic separations were carried out using silica gel 60 (Merck, 63–200 μm particle sized, 60–230 mesh). FTIR spectra were recorded as ATR on either a Thermo Scientific Nicolet 6700 spectrometer or Alpha T FTIR spectrometer or a Perkin Elmer Spectrum 100 Optical FTIR spectrometer. ^{1}H NMR and ^{13}C NMR spectra were obtained on either Varian^{UNITY} INOVA spectrometers with 500 MHz frequency for ^{1}H and 125 MHz frequency for ^{13}C NMR in ppm (δ) or Bruker spectrometers with 400 MHz frequency for ^{1}H and 100 MHz frequency for ^{13}C NMR in ppm (δ). ^{1}H NMR spectra and ^{13}C NMR spectra in $CDCl_3$ refer to the solvent signal center at δ 7.19 and δ 76.0 ppm, respectively. Chemical shifts (δ) are reported in parts per million (ppm). Coupling constants (J) are reported in Hz. Standard abbreviations indicating multiplicity were used as follows: *s* (singlet), *br s* (broad singlet), *d* (doublet), *t* (triplet), *q* (quartet), *sext* (sextet), *m* (multiplet), *dd* (doublet of doublets), *dt* (doublet of triplets), and *td* (triplet of doublets). Mass spectra were obtained on either a Thermo Finnigan LCQ Advantage MAX MS/MS spectrometer equipped with an ESI (Electrospray ionization) sources or a BRUKER Microflex LT by MALDI (Matrix Assisted Laser Desorption Ionization)-TOF technique *via* addition of 1,8,9-anthracenetriol (DIT, dithranol) as matrix. Data for the single crystal compounds were obtained with Bruker APEX II QUAZAR three-circle diffractometer. Indexing was performed using APEX2 [64]. Data integration and reduction were carried out with SAINT [65]. Absorption correction was performed by multi-scan method implemented in SADABS [66]. The Bruker SHELXTL [67] software package was used for structures solution and structures refinement. Aromatic C-bound and *N*-bound hydrogen atoms were positioned geometrically and refined using a riding mode. Crystal structure validations and geometrical calculations were performed using the Platon software [68]. Mercury software [69] was used for visualization of the .cif files. 2,3-Dimethyl-1,4-benzoquinone (**2**) was synthesized using the reported method in the literature [57].

4.2. General synthetic procedure 1: For the preparation of PQ analogs [59]

A suspension of the appropriate substituted aniline (4.40 mmol, 1.2 equiv.) and 2,3-dimethyl-1,4-benzoquinone (**2**, 0.500 g, 3.67 mmol) in absolute EtOH (25 mL) was stirred at reflux for 6–12 h until the consumption of the quinone. The reaction was monitored by TLC until the spot of starting materials disappeared under UV light. The reaction

mixture was cooled to ambient temperature. After evaporation of the solvent, the residue was dissolved with CH_2Cl_2 (3 × 50 mL), and the solution was washed sequentially with water (3 × 30 mL). The organic layers were collected, dried over anhydrous $CaCl_2$, filtered, concentrated under reduced pressure, and purified by means of column chromatography on silica gel to afford the pure compounds.

4.3. General synthetic procedure 2: One-pot reaction for the preparation of PQ analogs [60]

In a round-bottom flask, the corresponding substituted aniline (4.00 mmol, 2 equiv.) and 2,3-dimethylhydroquinone (**1**, 0.276 g, 2.00 mmol) was suspended in MeOH (12 mL). To a stirred the mixture was added sodium iodate (6.00 mmol, 3 equiv.) in water (12 mL) at room temperature for 12–24 h. The reaction was monitored by TLC until the spot of starting materials disappeared under UV light. After evaporation of the solvent, the residue was extracted with CH_2Cl_2 (3 × 50 mL), and the combined organic layers were washed with water (3 × 50 mL). Finally, the organic layer was dried with anhydrous $CaCl_2$ and concentrated under vacuum. The residue was purified by column chromatography on silica gel to give the pure compounds.

4.3.1. 5-((2-Methoxyphenyl)amino)-2,3-dimethyl-1,4-benzoquinone (PQ1)

Following the general synthetic procedure 1 by applying 2-methoxyaniline (0.542 g, 4.40 mmol), the crude residue was purified by column chromatography to furnish **PQ1** as a dark red solid. Yield: 49%, mp 170–172 °C. FTIR (ATR) υ (cm^{-1}): 3300 (NH), 3011 ($CH_{aromatic}$), 2959, 2919, 2848 ($CH_{aliphatic}$), 1666 (> C═O). ^{1}H NMR (400 MHz, *CDCl$_3$*) δ (ppm): 1.99–2.00 (m, 6H, CH_3), 3.83 (s, 3H, OCH_3), 6.16 (s, 1H, CH), 6.85–6.93 (m, 2H, $CH_{aromatic}$), 7.00–7.05 (m, 1H, $CH_{aromatic}$), 7.28 (dd, *J* = 7.9 and 1.5 Hz, 1H, $CH_{aromatic}$), 7.75 (br s, 1H, NH). ^{13}C NMR (100 MHz, *CDCl$_3$*) δ (ppm): 12.1, 12.8 (CH_3), 55.8 (OCH_3), 100.9, 111.0, 120.2, 120.9, 124.8, 127.5, 136.8, 141.9, 143.8, 150.8 ($C_{aromatic}$ and C_q), 184.1, 186.6 (> C═O). MS (+ESI) *m/z* (%): 259 (15, $[M + 2H]^+$), 258 (100, $[M + H]^+$). Anal. Calcd. for $C_{15}H_{15}NO_3$ (257.28).

4.3.2. 5-((3-Methoxyphenyl)amino)-2,3-dimethyl-1,4-benzoquinone (PQ2) [61]

Following the general synthetic procedure 1 by applying 3-methoxyaniline (0.542 g, 4.40 mmol), the crude residue was purified by column chromatography to furnish **PQ2** as a claret red solid. Yield: 16%, mp 142–143 °C. FTIR (ATR) υ (cm^{-1}): 3337 (NH), 3063 ($CH_{aromatic}$), 2922, 2852 ($CH_{aliphatic}$), 1664 (> C═O). ^{1}H NMR (400 MHz, *CDCl$_3$*) δ (ppm): 1.98–1.99 (m, 6H, CH_3), 3.74 (s, 3H, OCH_3), 6.11 (s, 1H, CH), 6.62–6.66 (m, 2H, $CH_{aromatic}$), 6.72 (dd, *J* = 8.0 and 1.6 Hz, 1H, $CH_{aromatic}$), 7.20 (t, *J* = 8.1 Hz, 1H, $CH_{aromatic}$), 7.25 (br s, 1H, NH). ^{13}C NMR (100 MHz, *CDCl$_3$*) δ (ppm): 12.1, 12.8 (CH_3), 55.4 (OCH_3), 101.2, 107.8, 110.4, 114.2, 130.4, 136.7, 139.0, 142.4, 143.9, 160.6 ($C_{aromatic}$ and C_q), 184.0, 186.6 (> C═O). MS (+ESI) *m/z* (%): 259 (23, $[M + 2H]^+$), 258 (100, $[M + H]^+$), 257 (4, $[M]^+$). Anal. Calcd. for $C_{15}H_{15}NO_3$ (257.28).

4.3.3. 5-((4-Methoxyphenyl)amino)-2,3-dimethyl-1,4-benzoquinone (PQ3)

Following the general synthetic procedure 1 by applying 4-methoxyaniline (0.542 g, 4.40 mmol), the crude residue was purified by column chromatography to furnish **PQ3** as a dark purple solid. Yield: 28%, mp 103–104 °C. FTIR (ATR) υ (cm^{-1}): 3293 (NH), 3010 ($CH_{aromatic}$), 2932, 2834 ($CH_{aliphatic}$), 1660 (> C═O). ^{1}H NMR (500 MHz, *CDCl$_3$*) δ (ppm): 1.93–1.97 (m, 6H, CH_3), 3.72 (s, 3H, OCH_3), 5.85 (s, 1H, CH), 6.81 (dt, *J* = 9.3 and 2.4 Hz, 2H, $CH_{aromatic}$), 7.03 (dt, *J* = 8.8 and 2.0 Hz, 2H, $CH_{aromatic}$), 7.15 (br s, 1H, NH). ^{13}C NMR (125 MHz, *CDCl$_3$*) δ (ppm): 12.2, 13.0 (CH_3), 55.8 (OCH_3), 99.9, 115.0, 124.5, 130.8, 136.6, 143.8, 144.2, 157.5 ($C_{aromatic}$ and C_q), 184.3, 186.5 (> C═O). MS (-ESI) *m/z* (%): 257 (16, $[M]^-$), 256 (100, $[M-H]^-$). Anal. Calcd. for $C_{15}H_{15}NO_3$ (257.28).

4.3.4. 5-((2-Ethoxyphenyl)amino)-2,3-dimethyl-1,4-benzoquinone (PQ4)

Following the general synthetic procedure 1 by applying 2-ethoxyaniline (0.604 g, 4.40 mmol), the crude residue was purified by column chromatography to furnish **PQ4** as a dark red solid. Yield: 16%, mp 116–117 °C. FTIR (ATR) υ (cm^{-1}): 3302 (NH), 2992, 2944 ($CH_{aliphatic}$), 1644 (> C═O). ^{1}H NMR (400 MHz, *CDCl$_3$*) δ (ppm): 1.39 (t, *J* = 7.0 Hz, 3H, CH_3), 1.96–1.98 (m, 6H, CH_3), 4.02 (q, *J* = 7.0 Hz, 2H, OCH_2), 6.16 (s, 1H, CH), 6.79–6.90 (m, 2H, $CH_{aromatic}$), 6.97 (td, *J* = 7.8 and 1.6 Hz, 1H, $CH_{aromatic}$), 7.25 (dd, *J* = 7.9 and 1.5 Hz, 1H, $CH_{aromatic}$), 7.85 (br s, 1H, NH). ^{13}C NMR (100 MHz, *CDCl$_3$*) δ (ppm): 12.1, 12.8, 14.8 (CH_3), 64.3 (OCH_2), 101.0, 111.9, 119.7, 120.7, 124.6, 127.7, 136.7, 141.6, 143.8, 149.9 ($C_{aromatic}$ and C_q), 184.1, 186.5 (> C═O). MS (MALDI TOF) *m/z*: 271 $[M]^+$. Anal. Calcd. for $C_{16}H_{17}NO_3$ (271.31).

4.3.5. 5-((3-Ethoxyphenyl)amino)-2,3-dimethyl-1,4-benzoquinone (PQ5)

Following the general synthetic procedure 1 by applying 3-ethoxyaniline (0.604 g, 4.40 mmol), the crude residue was purified by column chromatography to furnish **PQ5** as a dark red solid. Yield: 6%, mp 99–100 °C. FTIR (ATR) υ (cm^{-1}): 3328 (NH), 2987, 2921 ($CH_{aliphatic}$), 1640 (> C═O). ^{1}H NMR (400 MHz, *CDCl$_3$*) δ (ppm): 1.35 (t, *J* = 7.0 Hz, 3H, CH_3), 1.98–2.00 (m, 6H, CH_3), 3.95 (q, *J* = 7.0 Hz, 2H, OCH_2), 6.12 (s, 1H, CH), 6.58–6.72 (m, 3H, $CH_{aromatic}$), 7.19 (t, *J* = 8.1 Hz, 1H, $CH_{aromatic}$), 7.24 (br s, 1H, NH). ^{13}C NMR (100 MHz, *CDCl$_3$*) δ (ppm): 12.1, 12.8, 14.8 (CH_3), 63.7 (OCH_2), 101.1, 108.3, 111.0, 114.0, 130.3, 136.7, 139.0, 142.4, 143.9, 160.0 ($C_{aromatic}$ and C_q), 184.0, 186.6 (> C═O). MS (MALDI TOF) *m/z*: 271 $[M]^+$. Anal. Calcd. for $C_{16}H_{17}NO_3$ (271.31).

4.3.6. 5-((4-Ethoxyphenyl)amino)-2,3-dimethyl-1,4-benzoquinone (PQ6)

Following the general synthetic procedure 1 by applying 4-ethoxyaniline (0.604 g, 4.40 mmol), the crude residue was purified by column chromatography to furnish **PQ6** as a brown solid. Yield: 19%, mp 107–109 °C. FTIR (ATR) υ (cm^{-1}): 3312 (NH), 3050 ($CH_{aromatic}$), 2977, 2929 ($CH_{aliphatic}$), 1655 (> C═O). ^{1}H NMR (500 MHz, *CDCl$_3$*) δ (ppm): 1.34 (t, *J* = 6.8 Hz, 3H, CH_3), 1.95–1.99 (m, 6H, CH_3), 3.95 (q, *J* = 6.8 Hz, 2H, OCH_2), 5.87 (s, 1H, CH), 6.82 (dt, *J* = 9.3 and 2.4 Hz, 2H, $CH_{aromatic}$), 7.03 (dt, *J* = 8.8 and 2.0 Hz, 2H, $CH_{aromatic}$), 7.11 (br s, 1H, NH). ^{13}C NMR (125 MHz, *CDCl$_3$*) δ (ppm): 11.0, 11.8, 13.8 (CH_3), 62.8 (OCH_2), 98.7, 114.3, 123.3, 129.3, 135.4, 142.6, 143.1, 155.7 ($C_{aromatic}$ and C_q), 183.1, 185.3 (> C═O). MS (+ESI) *m/z* (%): 273 (16, $[M + 2H]^+$), 272 (100, $[M + H]^+$); MS (-ESI) *m/z* (%): 271 (9, $[M]^-$), 270 (100, $[M-H]^-$). Anal. Calcd. for $C_{16}H_{17}NO_3$ (271.31).

4.3.7. 5-((4-Butoxyphenyl)amino)-2,3-dimethyl-1,4-benzoquinone (PQ7)

Following the general synthetic procedure 1 by applying 4-butoxyaniline (0.727 g, 4.40 mmol), the crude residue was purified by column chromatography to furnish **PQ7** as a purple solid. Yield: 8%, mp 87–88 °C. FTIR (ATR) υ (cm^{-1}): 3261 (NH), 2957, 2923, 2871 ($CH_{aliphatic}$), 1664 (> C═O). ^{1}H NMR (500 MHz, *CDCl$_3$*) δ (ppm): 0.90 (t, *J* = 7.3 Hz, 3H, CH_3), 1.42 (sext, *J* = 7.3 Hz, 2H, CH_2CH_3), 1.66–1.72 (m, 2H, OCH_2CH_2), 1.96 (s, 3H, CH_3), 1.97 (s, 3H, CH_3), 3.88 (t, *J* = 6.3 Hz, 2H, OCH_2), 5.87 (s, 1H, CH), 6.81 (d, *J* = 8.8 Hz, 2H, $CH_{aromatic}$), 7.02 (d, *J* = 8.8 Hz, 2H, $CH_{aromatic}$), 7.12 (br s, 1H, NH). ^{13}C NMR (125 MHz, *CDCl$_3$*) δ (ppm): 11.0, 11.8, 12.8 (CH_3), 18.2, 30.3 (CH_2), 67.0 (OCH_2), 98.5, 114.4, 123.1, 129.3, 135.4, 142.6, 143.0, 155.9 ($C_{aromatic}$ and C_q), 183.1, 185.3 (> C═O). MS (-ESI) *m/z* (%): 301 (3, $[M + 2H]^-$), 299 (12, $[M]^-$), 298 (100, $[M-H]^-$). Anal. Calcd. for $C_{18}H_{21}NO_3$ (299.36).

4.3.8. 5-((2,4-Dimethoxyphenyl)amino)-2,3-dimethyl-1,4-benzoquinone (PQ8) [62]

Following the general synthetic procedure 2 by applying 2,4-

dimethoxyaniline (0.612 g, 4.00 mmol) and sodium iodate (1.186 g, 6.00 mmol), the crude residue was purified by column chromatography to furnish **PQ8** as a dark purple solid. Yield: 40%, mp 126–128 °C. FTIR (ATR) υ (cm^{-1}): 3318 (NH), 2934 ($CH_{aliphatic}$), 1644 (> C=O). ^{1}H NMR (400 MHz, *CDCl$_3$*) δ (ppm): 1.98–1.99 (m, 6H, CH_3), 3.75 (s, 3H, OCH_3), 3.79 (s, 3H, OCH_3), 5.97 (s, 1H, CH), 6.39–6.46 (m, 2H, $CH_{aromatic}$), 7.15 (d, *J* = 8.7 Hz, 1H, $CH_{aromatic}$), 7.46 (br s, 1H, NH). ^{13}C NMR (100 MHz, *CDCl$_3$*) δ (ppm): 11.0, 11.8 (CH_3), 54.6, 54.7 (OCH_3), 98.4, 98.7, 102.9, 119.4, 121.1, 135.5, 141.6, 143.0, 151.5, 156.7 ($C_{aromatic}$ and C_q), 183.2, 185.4 (> C=O). MS (MALDI TOF) *m/z*: 287 $[M]^+$. Anal. Calcd. for $C_{16}H_{17}NO_4$ (287.31).

4.3.9. 5-((2,5-Dimethoxyphenyl)amino)-2,3-dimethyl-1,4-benzoquinone (PQ9)

Following the general synthetic procedure 2 by applying 2,5-dimethoxyaniline (0.612 g, 4.00 mmol) and sodium iodate (1.186 g, 6.00 mmol), the crude residue was purified by column chromatography to furnish **PQ9** as a purple solid. Yield: 6%, mp 104–106 °C. FTIR (ATR) υ (cm^{-1}): 3295 (NH), 2920, 2849 ($CH_{aliphatic}$), 1646 (> C=O). ^{1}H NMR (500 MHz, *CDCl$_3$*) δ (ppm): 1.98–2.01 (m, 6H, CH_3), 3.71 (s, 3H, OCH_3), 3.78 (s, 3H, OCH_3), 6.19 (s, 1H, CH), 6.53 (dd, *J* = 8.9 and 2.9 Hz, 1H, $CH_{aromatic}$), 6.77 (d, *J* = 8.9 Hz, 1H, $CH_{aromatic}$), 6.87 (d, *J* = 2.8 Hz, 1H, $CH_{aromatic}$), 7.78 (br s, 1H, NH). ^{13}C NMR (125 MHz, *CDCl$_3$*) δ (ppm): 12.1, 12.8 (CH_3), 55.8, 56.3 (OCH_3), 101.4, 107.2, 108.3, 111.5, 128.2, 136.8, 141.5, 143.8, 145.0, 153.8 ($C_{aromatic}$ and C_q), 184.0, 186.5 (> C=O). MS (MALDI TOF) *m/z*: 287 $[M]^+$. Anal. Calcd. for $C_{16}H_{17}NO_4$ (287.31).

4.3.10. 5-((3,4-Dimethoxyphenyl)amino)-2,3-dimethyl-1,4-benzoquinone (PQ10)

Following the general synthetic procedure 2 by applying 3,4-dimethoxyaniline (0.612 g, 4.00 mmol) and sodium iodate (1.186 g, 6.00 mmol), the crude residue was purified by column chromatography to furnish **PQ10** as a purple solid. Yield: 62%, mp 151–153 °C. FTIR (ATR) υ (cm^{-1}): 3341 (NH), 3070, 3014 ($CH_{aromatic}$), 2961 ($CH_{aliphatic}$), 1640 (> C=O). ^{1}H NMR (400 MHz, *CDCl$_3$*) δ (ppm): 1.98–2.00 (m, 6H, CH_3), 3.81 (s, 3H, OCH_3), 3.82 (s, 3H, OCH_3), 5.93 (s, 1H, CH), 6.64 (d, *J* = 2.4 Hz, 1H, $CH_{aromatic}$), 6.70 (dd, *J* = 8.6 and 2.4 Hz, 1H, $CH_{aromatic}$), 6.79 (d, *J* = 8.6 Hz, 1H, $CH_{aromatic}$), 7.14 (br s, 1H, NH). ^{13}C NMR (100 MHz, *CDCl$_3$*) δ (ppm): 11.0, 11.8 (CH_3), 55.0, 55.1 (OCH_3), 98.9, 105.8, 110.6, 113.9, 129.7, 135.4, 142.4, 143.1, 145.9, 148.6 ($C_{aromatic}$ and C_q), 183.1, 185.3 (> C=O). MS (MALDI TOF) *m/z*: 287 $[M]^+$. Anal. Calcd. for $C_{16}H_{17}NO_4$ (287.31).

4.3.11. 5-((3,5-Dimethoxyphenyl)amino)-2,3-dimethyl-1,4-benzoquinone (PQ11)

Following the general synthetic procedure 2 by applying 3,5-dimethoxyaniline (0.612 g, 4.00 mmol) and sodium iodate (1.186 g, 6.00 mmol), the crude residue was purified by column chromatography to furnish **PQ11** as a purple solid. Yield: 27%, mp 142–144 °C. FTIR (ATR) υ (cm^{-1}): 3349 (NH), 3050 ($CH_{aromatic}$), 2922, 2850 ($CH_{aliphatic}$), 1640 (> C=O). ^{1}H NMR (400 MHz, *CDCl$_3$*) δ (ppm): 1.98–2.00 (m, 6H, CH_3), 3.72 (s, 6H, OCH_3), 6.13 (s, 1H, CH), 6.19 (t, *J* = 2.1 Hz, 1H, $CH_{aromatic}$), 6.27 (d, *J* = 2.1 Hz, 2H, $CH_{aromatic}$), 7.21 (br s, 1H, NH). ^{13}C NMR (100 MHz, *CDCl$_3$*) δ (ppm): 11.1, 11.8 (CH_3), 54.4, 54.5 (OCH_3), 96.0, 99.2, 100.5, 135.6, 138.5, 141.3, 142.8, 160.5 ($C_{aromatic}$ and C_q), 182.9, 185.5 (> C=O). MS (MALDI TOF) *m/z*: 288 $[M + H]^+$. Anal. Calcd. for $C_{16}H_{17}NO_4$ (287.31).

4.3.12. 5-((2,5-Diethoxyphenyl)amino)-2,3-dimethyl-1,4-benzoquinone (PQ12)

Following the general synthetic procedure 1 by applying 2,5-diethoxyaniline (0.798 g, 4.40 mmol), the crude residue was purified by column chromatography to furnish **PQ12** as a purple solid. Yield: 37%, mp 69–71 °C. FTIR (ATR) υ (cm^{-1}): 3223 (NH), 2973, 2928 ($CH_{aliphatic}$), 1645 (> C=O). ^{1}H NMR (500 MHz, *CDCl$_3$*) δ (ppm): 1.33 (t, *J* = 6.8 Hz, 3H, OCH_2CH_3), 1.37 (t, *J* = 6.8 Hz, 3H, OCH_2CH_3), 2.00 (m, 6H, CH_3), 3.91 (q, *J* = 7.3 Hz, 2H, OCH_2), 3.98 (q, *J* = 7.3 Hz, 2H, OCH_2), 6.22 (s, 1H, CH), 6.49 (dd, *J* = 9.3 and 2.9 Hz, 1H, $CH_{aromatic}$), 6.75 (d, *J* = 9.3 Hz, 1H, $CH_{aromatic}$), 6.87 (d, *J* = 2.9 Hz, 1H, $CH_{aromatic}$), 7.90 (br s, 1H, NH). ^{13}C NMR (125 MHz, *CDCl$_3$*) δ (ppm): 12.1, 12.8, 14.8, 14.9 (CH_3), 64.2, 65.0 (OCH_2), 101.3, 107.3, 108.9, 112.9, 128.6, 136.8, 141.4, 143.8, 144.1, 153.1 ($C_{aromatic}$ and C_q), 184.0, 186.5 (> C=O). MS (MALDI TOF) *m/z*: 315 $[M]^+$. Anal. Calcd. for $C_{18}H_{21}NO_4$ (315.36).

4.3.13. 5-(Benzo[d] [1,3]dioxol-5-ylamino)-2,3-dimethyl-1,4-benzoquinone (PQ13)

Following the general synthetic procedure 2 by applying 3,4-(methylenedioxy)aniline (0.548 g, 4.00 mmol) and sodium iodate (1.186 g, 6.00 mmol), the crude residue was purified by column chromatography to furnish **PQ13** as a purple solid. Yield: 8%, mp 165–166 °C. FTIR (ATR) υ (cm^{-1}): 3332 (NH), 2922, 2854 ($CH_{aliphatic}$), 1640 (> C=O). ^{1}H NMR (400 MHz, *CDCl$_3$*) δ (ppm): 1.97–1.99 (m, 6H, CH_3), 5.90 (s, 1H, CH), 5.93 (s, 2H, OCH_2O), 6.58 (dd, *J* = 8.3 and 2.2 Hz, 1H, $CH_{aromatic}$), 6.65 (d, *J* = 2.2 Hz, 1H, $CH_{aromatic}$), 6.73 (d, *J* = 8.3 Hz, 1H, $CH_{aromatic}$), 7.08 (br s, 1H, NH). ^{13}C NMR (100 MHz, *CDCl$_3$*) δ (ppm): 12.1, 12.8 (CH_3), 100.1 (OCH_2O), 101.7, 104.5, 108.7, 116.3, 131.6, 136.5, 143.5, 144.0, 145.4, 148.4 ($C_{aromatic}$ and C_q), 184.1, 186.4 (> C=O). MS (MALDI TOF) *m/z*: 271 $[M]^+$. Anal. Calcd. for $C_{15}H_{13}NO_4$ (271.27).

4.3.14. 5-((2,3-Dihydrobenzo[b] [1,4]dioxin-6-yl)amino)-2,3-dimethyl-1,4-benzoquinone (PQ14)

Following the general synthetic procedure 2 by applying 1,4-benzodioxan-6-amine (0.604 g, 4.00 mmol) and sodium iodate (1.186 g, 6.00 mmol), the crude residue was purified by column chromatography to furnish **PQ14** as a dark purple solid. Yield: 12%, mp 148–150 °C. FTIR (ATR) υ (cm^{-1}): 3332 (NH), 1636 (> C=O). ^{1}H NMR (400 MHz, *CDCl$_3$*) δ (ppm): 1.94–1.98 (m, 6H, CH_3), 4.18 (s, 4H, OCH_2), 5.93 (s, 1H, CH), 6.59 (dd, *J* = 8.6 and 2.6 Hz, 1H, $CH_{aromatic}$), 6.65 (d, *J* = 2.6 Hz, 1H, $CH_{aromatic}$), 6.77 (d, *J* = 8.6 Hz, 1H, $CH_{aromatic}$), 7.11 (br s, 1H, NH). ^{13}C NMR (100 MHz, *CDCl$_3$*) δ (ppm): 12.1, 12.8 (CH_3), 64.3, 64.4 (OCH_2), 100.0, 111.8, 116.0, 117.9, 131.2, 136.5, 141.3, 143.2, 143.9, 144.0 ($C_{aromatic}$ and C_q), 184.1, 186.4 (> C=O). MS (MALDI TOF) *m/z*: 285 $[M]^+$. Anal. Calcd. for $C_{16}H_{15}NO_4$ (285.29).

4.3.15. 5-((3,4,5-Trimethoxyphenyl)amino)-2,3-dimethyl-1,4-benzoquinone (PQ15)

Following the general synthetic procedure 2 by applying 3,4,5-trimethoxyaniline (0.732 g, 4.00 mmol) and sodium iodate (1.186 g, 6.00 mmol), the crude residue was purified by column chromatography to furnish **PQ15** as a dark purple solid. Yield: 39%, mp 89–90 °C. FTIR (ATR) υ (cm^{-1}): 3264 (NH), 3011 ($CH_{aromatic}$), 2940 ($CH_{aliphatic}$), 1644 (> C=O). ^{1}H NMR (400 MHz, *CDCl$_3$*) δ (ppm): 1.98–2.00 (m, 6H, CH_3), 3.77 (s, 3H, OCH_3), 3.78 (s, 6H, OCH_3), 6.01 (s, 1H, CH), 6.35 (s, 2H, $CH_{aromatic}$), 7.16 (br s, 1H, NH). ^{13}C NMR (100 MHz, *CDCl$_3$*) δ (ppm): 12.1, 12.9 (CH_3), 56.3, 61.0 (OCH_3), 100.1, 100.7, 133.6, 135.7, 136.6, 142.9, 144.1, 153.9 ($C_{aromatic}$ and C_q), 184.0, 186.4 (> C=O). MS (MALDI TOF) *m/z*: 317 $[M]^+$. Anal. Calcd. for $C_{17}H_{19}NO_5$ (317.34).

4.4. Cell culture and MTT assay

4.4.1. Cell culture and drug treatment

Briefly, the K562, Jurkat, and MT-2 leukemic cell lines were cultured in RPMI 1640 (Wako Pure Chemical Industries, Osaka, Japan) medium with 10% fetal bovine serum (FBS) (Equitech-Bio, Texas, U.S.). Peripheral blood mononuclear cells (PBMC) (Precision Bioservices, Frederic, MD) were incubated in RPMI 1640 medium with 10% human serum AB (HS) (Gemini, Woodland, CA). All media were supplemented with 89 μM/mL streptomycin (Meiji Seika Pharma, Tokyo, Japan) in a humid atmosphere at 37 °C and 5% CO_2. In experiments, the leukemia

and PBMC cells were incubated in 24-well and 96-well culture plates (Iwaki brand Asahi Glass Co., Chiba, Japan) at 2×10^4 and 10^6 cells/mL concentration respectively for 24 h. The stock solution of compounds and Imatinib (Wako Pure Chemical Industries, Osaka, Japan) in concentrations between 3 and 30 mM were prepared in dimethyl sulfoxide (DMSO; Wako Pure Chemical Industries) and then were added to fresh culture medium. The concentration of DMSO in the final culture medium was 1%.

4.4.2. Cytotoxicity assay

The MTT test was performed as previously described in the literature with small modifications [70]. The tested compounds were cultured with cells in different concentrations (3–300 μM) for 24 h and then, MTT (Dojindo Molecular Technologies, Kumamoto, Japan) was added to cells. After 4 h of incubation, the medium was taken out and 100 μL DMSO was added to each well. The absorbance at 550 nm was measured using a microplate reader Infinitive M1000 (Tecan, Groding, Austria) with background subtraction at 630 nm. All experiments were run in triplicate and IC_{50} values were estimated from the results of the MTT test described as the drug concentrations that reduced absorbance to 50% of control values.

4.4.3. Detection of cell death

Apoptotic/necrotic/healthy detection kit (PromoKine, Heidelberg, Germany) was performed according to PromoKine's instructions with the modifications [71]. Briefly, K562 cells were treated with **PQ2** and Imatinib at IC_{50} concentrations for 6 h. Then, the cells were harvested and washed with PBS and stained with 4 μL of FITC-Annexin V, 4 μL of ethidium homodimer III and 4 μL of Hoechst 33,342 in 1 × binding buffer for 30 min at room temperature in the dark. The cells were analyzed by a fluorescence microscope Biorevo Fluorescence BZ-9000 (Keyence, Osaka, Japan). The number of apoptotic cells (Annexin V), late apoptotic or necrotic cells (Annexin V and Ethidium homodimer III) and necrotic cells (Ethidium homodimer III) were counted as previously described [72].

4.4.4. Kinase selectivity profiling assay

The kinase inhibition assay system (TK-2) (Promega Corporation, Madison, WI, USA) was performed as previously described with some modification [15]. In this system, eight kinase strips (Abl1, BRK, BTK, CSK, FYN A, LCK, LYN B, and SRC) and their substrates were diluted with 2.5x kinase reaction buffer (95 μL) and 100 μM ATP (15 μL) solution respectively. The reaction of kinases was performed in the 384-well plate using 2 μL of compound solution at multiple concentrations in a buffer, 4 μL of kinase working stock and 4 μL of ATP/substrate working stock. After 1 h of incubation at room temperature, the ADP-Glo Kinase Assay (Promega) protocol was employed and inhibitory kinase activity of the test compounds were determined as previously described [15].

4.4.5. Immunoblot analysis

The K562 cells were incubated in the presence of 5, 10, and 20 μM of **PQ2** and Imatinib for 6 h and then lysed in PBS-Laemmli sample buffer. Immunoblot analysis using phospho-specific-p44/42 MAPK (Erk1/2) (Thr202/Tyr204) (D13.14.4E) XP Rabbit mAb (1:1000) (from Cell Signaling Technology) or anti-β-actin clone AC-15 (from Sigma-Aldrich) was conducted. For immunoreactivity detection, Chemiluminescence method was performed [73].

4.4.6. DNA-cleaving activity

The DNA cleavage assay was performed as described previously [74].

4.4.7. Molecular docking simulation and ADMET prediction

Crystal structure of the Abl kinase domain in complex with Imatinib was retrieved from the RCSB Brookhaven Protein Data Bank (PDB: 1IEP); **PQ2** was built by ChemDraw Professional 15.1. Before docking simulations, **PQ2** and 1IEP were prepared as previously described [75]. MOE 2018.01 software (Chemical Computing Group, Montreal, Canada) was employed for preparation, interactive docking, visualization, and analysis procedures using its default parameters [76,77]. The ADMET properties were calculated *in silico* using ADMET predict 9 from Simulation Plus, Inc.; the risk models were previously explained in details [78].

Declaration of Competing Interest

The authors declare no conflict of interest.

Acknowledgements

This work was financially supported by the Scientific Research Projects Coordination Unit of Istanbul University-Cerrahpasa, Turkey (Project number: FBA-2017-24559) and the Grant-in-Aid for Challenging Exploratory Research (24659048) for supplying the equipment and materials. The crystallographic data have been deposited at the Cambridge Crystallographic Data Centre, and CCDC reference number are 1891326 for the **PQ1**, 1891328 for the **PQ4**, 1891330 for the **PQ11**, and 1891331 for the **PQ14**. The data can be obtained available free of charge from http://www.ccdc.cam.ac.uk/conts/retrieving.html or from the Cambridge Crystallographic Data Centre (CCDC), 12 Union Road, Cambridge CB2 1EZ, UK; fax: +44 (0) 1223336033; email: deposit@ccdc.cam.ac.uk. We also thank Sadık Metin Ceyhan and Yunus Zorlu for helpful discussions on crystal structure analyses.

Appendix A. Supplementary material

Supplementary data to this article can be found online at https://doi.org/10.1016/j.bioorg.2019.103255.

References

[1] WHO, Monitoring Health for The Sustainable Development Goals, World Health Organization Geneva (Switzerland) (2017).
[2] WHO, Cancer Fact sheet, World Health Organization Geneva (Switzerland) (2017).
[3] WHO, Cancer Country Profiles, World Health Organization Geneva (Switzerland) (2014).
[4] G.N. Wogan, S.S. Hecht, J.S. Felton, A.H. Conney, L.A. Loeb, Environmental and chemical carcinogenesis, Semin. Cancer Biol. 14 (2004) 473–486.
[5] R.K. Saini, R. Chouhan, L.P. Bagri, A.K. Bajpai, Strategies of targeting tumors and cancers, J. Cancer Res. Updates 1 (2012) 129–152.
[6] K.W. Wellington, Understanding cancer and the anticancer activities of naphthoquinones - a review, RSC Adv. 5 (26) (2015) 20309–20338.
[7] L. Brannon-Peppas, J.O. Blanchette, Nanoparticle and targeted systems for cancer therapy, Adv. Drug Deliv. Rev. 56 (11) (2004) 1649–1659.
[8] V.T. DeVita, E. Chu, A history of cancer chemotherapy, Cancer Res. 68 (21) (2008) 8643–8653.
[9] R.K. Jain, Barriers to drug-delivery in solid tumors, Sci. Am. 271 (1) (1994) 58–65.
[10] D. Hanahan, R.A. Weinberg, Hallmarks of cancer: the next generation, Cell 144 (5) (2011) 646–674.
[11] J. Xu, X. Zhang, H. Yang, G. Ding, B. Jin, Y. Lou, Y. Zhang, H. Wang, B. Han, Comparison of outcomes of tyrosine kinase inhibitor in first- or second-line therapy for advanced non-small-cell lung cancer patients with sensitive EGFR mutations, Oncotarget 7 (42) (2016) 68442–68448.
[12] D.R. Knighton, J.H. Zheng, L.F. Ten Eyck, V.A. Ashford, N.H. Xuong, S.S. Taylor, J.M. Sowadski, Crystal structure of the catalytic subunit of cyclic adenosine monophosphate-dependent protein kinase, Science 253 (5018) (1991) 407–414.
[13] C. Gambacorti-Passerini, R. Piazza, Imatinib–a new tyrosine kinase inhibitor for first-line treatment of chronic myeloid leukemia in 2015, Jama Oncol. 1 (2) (2015) 143–144.
[14] N.P. van Erp, H. Gelderblom, H.J. Guchelaar, Clinical pharmacokinetics of tyrosine kinase inhibitors, Cancer Treat. Rev. 35 (8) (2009) 692–706.
[15] H.I. Ciftci, S.E. Ozturk, T.F.S. Ali, M.O. Radwan, H. Tateishi, R. Koga, Z. Ocak, M. Can, M. Otsuka, M. Fujita, The first pentacyclic triterpenoid gypsogenin derivative exhibiting anti-ABL1 kinase and anti-chronic myelogenous leukemia activities, Biol. Pharm. Bull. 41 (4) (2018) 570–574.
[16] J.V. Melo, C. Chuah, Resistance to imatinib mesylate in chronic myeloid leukaemia, Cancer Lett. 249 (2) (2007) 121–132.
[17] E. Weisberg, P.W. Manley, S.W. Cowan-Jacob, A. Hochhaus, J.D. Griffin, Second

generation inhibitors of BCR-ABL for the treatment of imatinib-resistant chronic myeloid leukaemia, Nat. Rev. Cancer 7 (5) (2007) 345–356.
[18] X. An, A.K. Tiwari, Y. Sun, P.R. Ding, C.R. Ashby Jr., Z.S. Chen, BCR-ABL tyrosine kinase inhibitors in the treatment of Philadelphia chromosome positive chronic myeloid leukemia: a review, Leuk. Res. 34 (10) (2010) 1255–1268.
[19] G.M. Cragg, P.G. Grothaus, D.J. Newman, Impact of natural products on developing new anti-cancer agents, Chem. Rev. 109 (7) (2009) 3012–3043.
[20] D.J. Newman, G.M. Cragg, Natural products as sources of new drugs over the last 25 years, J. Nat. Prod. 70 (3) (2007) 461–477.
[21] M.S. Butler, Natural products to drugs: natural product-derived compounds in clinical trials, Nat. Prod. Rep. 25 (3) (2008) 475–516.
[22] T. Henkel, R.M. Brunne, H. Muller, F. Reichel, Statistical investigation into the structural complementarity of natural products and synthetic compounds, Angew. Chem. Int. Ed. 38 (5) (1999) 643–647.
[23] N.P. Collett, A.R.M.R. Amin, S. Bayraktar, J.M. Pezzuto, D.M. Shin, F.R. Khuri, B.B. Aggarwal, Y.J. Surh, O. Kucuk, Cancer prevention with natural compounds, Semin. Oncol. 37 (3) (2010) 258–281.
[24] M. El-Dakhakhany, Studies on the chemical constitution of Egyptian N. sativa L. seeds, Planta Med. 11 (1963) 465–470.
[25] K. Sugiura, Antitumor activity of mitomycin C, Cancer Chemother. Rep. 13 (1961) 51–65.
[26] A. Begleiter, Clinical applications of quinone-containing alkylating agents, Front Biosci. 5 (2000) E153–E171.
[27] S. Banerjee, A.S. Azmi, S. Padhye, M.W. Singh, J.B. Baruah, P.A. Philip, F.H. Sarkar, R.M. Mohammad, Structure-activity studies on therapeutic potential of thymoquinone analogs in pancreatic cancer, Pharm. Res.-Dordr. 27 (6) (2010) 1146–1158.
[28] O.R. Johnson-Ajinwo, I. Ullah, H. Mbye, A. Richardson, P. Horrocks, W.W. Li, The synthesis and evaluation of thymoquinone analogues as anti-ovarian cancer and antimalarial agents, Bioorg. Med. Chem. Lett. 28 (7) (2018) 1219–1222.
[29] M. Kawamukai, Biosynthesis and applications of prenylquinones, Biosci. Biotech. Bioch. 82 (6) (2018) 963–977.
[30] N. Bayrak, H. Yildirim, A.F. Tuyun, E.M. Kara, B.O. Celik, G.K. Gupta, H.I. Ciftci, M. Fujita, M. Otsuka, H.R. Nasiri, Synthesis, computational study, and evaluation of in vitro antimicrobial, antibiofilm, and anticancer activities of new sulfanyl aminonaphthoquinone derivatives, Lett. Drug Des. Discov. 14 (6) (2017) 647–661.
[31] H. Yildirim, N. Bayrak, A.F. Tuyun, E.M. Kara, B.O. Celik, G.K. Gupta, 2,3-Disubstituted-1,4-naphthoquinones containing an arylamine with trifluoromethyl group: synthesis, biological evaluation, and computational study, RSC Adv. 7 (41) (2017) 25753–25764.
[32] E. Leyva, A. Cardenas-Chaparro, S.E. Loredo-Carrillo, L.I. Lopez, F. Mendez-Sanchez, A. Martinez-Richa, Ultrasound-assisted reaction of 1,4-naphthoquinone with anilines through an EDA complex, Mol. Divers. 22 (2) (2018) 281–290.
[33] A.J. Harvie, C.T. Smith, R. Ahumada-Lazo, L.J.C. Jeuken, M. Califano, R.S. Bon, S.J.O. Hardman, D.J. Binks, K. Critchley, Ultrafast trap state-mediated electron transfer for quantum dot redox sensing, J. Phys. Chem. C 122 (18) (2018) 10173–10180.
[34] C.Y. Sie, C.P. Chuang, Electrophilic carbocyclization reactions of 2-(2-alkynylphenyl)amino-1,4-naphthoquinones, Org. Biomol. Chem. 16 (30) (2018) 5483–5491.
[35] H.R. Lawrence, A. Kazi, Y.T. Luo, R. Kendig, Y.Y. Ge, S. Jain, K. Daniel, D. Santiago, W.C. Guida, S.M. Sebti, Synthesis and biological evaluation of naphthoquinone analogs as a novel class of proteasome inhibitors, Bioorg. Med. Chem. 18 (15) (2010) 5576–5592.
[36] A. Kacmaz, Z. Hamurcu, New NH-substituted 1,4-naphtho- and 1,4-benzo- quinones: Synthesis, characterization and potential antiproliferative effect against MDA-MB-231 cells, Phosphorus, Sulfur, and Silicon and the Related Elements, (2018).
[37] A. Kacmaz, E.T. Acar, G. Atun, K. Kaya, B.D. Sigirci, F. Bagcigil, Synthesis, electrochemistry, DFT calculations, antimicrobial properties and X-ray crystal structures of some NH- and/or S- substituted-1,4-quinones, Chem. Select 3 (30) (2018) 8615–8623.
[38] J. Benites, J.A. Valderrama, M. Ramos, G.G. Muccioli, P.B. Calderon, Targeting Akt as strategy to kill cancer cells using 3-substituted 5-anilinobenzo[c]isoxazolequinones: a preliminary study, Biomed. Pharmacother. 97 (2018) 778–783.
[39] H.Y. You, S.R. Vegi, C. Lagishetti, S. Chen, R.S. Reddy, X.H. Yang, J. Guo, C.H. Wang, Y. He, Synthesis of bioactive 3,4-dihydro-2H-naphtho[2,3-b][1,4]oxazine-5,10-dione and 2,3,4,5-tetrahydro-1H-naphtho[2,3-b]azepine-6,11-dione derivatives via the copper-catalyzed intramolecular coupling reaction, J. Org. Chem. 83 (7) (2018) 4119–4130.
[40] T.V. Baiju, R.G. Almeida, S.T. Sivanandan, C.A. de Simone, L.M. Brito, B.C. Cavalcanti, C. Pessoa, I.N.N. Namboothiri, E.N. da Silva, Quinonoid compounds via reactions of lawsone and 2-aminonaphthoquinone with alpha-bromonitroalkenes and nitroallylic acetates: structural diversity by C-ring modification and cytotoxic evaluation against cancer cells, Eur. J. Med. Chem. 151 (2018) 686–704.
[41] K. Li, B.T. Wang, L.F. Zheng, K. Yang, Y.Y. Li, M.M. Hu, D. He, Target ROS to induce apoptosis and cell cycle arrest by 5,7-dimethoxy-1,4-naphthoquinone derivative, Bioorg. Med. Chem. Lett. 28 (3) (2018) 273–277.
[42] A.K. Jordao, J. Novais, B. Leal, A.C. Escobar, H.M. dos Santos, H.C. Castro, V.F. Ferreira, Synthesis using microwave irradiation and antibacterial evaluation of new N, O-acetals and N, S-acetals derived from 2-amino-1,4-naphthoquinones, Eur. J. Med. Chem. 63 (2013) 196–201.
[43] M. Janeczko, O.M. Demchuk, D. Strzelecka, K. Kubinski, M. Maslyk, New family of antimicrobial agents derived from 1,4-naphthoquinone, Eur. J. Med. Chem. 124 (2016) 1019–1025.
[44] K.W. Wellington, N.B.P. Nyoka, L.J. McGaw, Investigation of the antibacterial and antifungal activity of thiolated naphthoquinones, Drug. Dev. Res. 1–9 (2019), https://doi.org/10.1002/ddr.21512.
[45] C.K. Ryu, S.Y. Oh, S.J. Choi, D.Y. Kang, Synthesis of antifungal evaluation of 2H-[1,2,3]triazolo[4,5-g]isoquinoline-4,9-diones, Chem. Pharm. Bull. 62 (11) (2014) 1119–1124.
[46] U. Glamoclija, S. Padhye, S. Spirtovic-Halilovic, A. Osmanovic, E. Veljovic, S. Roca, I. Novakovic, B. Mandic, I. Turel, J. Kljun, S. Trifunovic, E. Kahrovic, S. Kraljevic Pavelic, A. Harej, M. Klobucar, D. Zavrsnik, Synthesis biological evaluation and docking studies of benzoxazoles derived from thymoquinone, Molecules 23 (12) (2018).
[47] Y. Brandy, I. Ononiwu, D. Adedeji, V. Williams, C. Mouamba, Y. Kanaan, R.L. Copeland, D.A. Wright, R.J. Butcher, S.R. Denmeade, O. Bakare, Synthesis and cytotoxic activities of some 2-Arylnaphtho[2,3-d]oxazole-4,9-dione derivatives on androgen-dependent (LNCaP) and androgen-independent (PC3) human prostate cancer cell lines, Invest. New Drug. 30 (4) (2012) 1709–1714.
[48] K.W. Wellington, N.I. Kolesnikova, N.B.P. Nyoka, L.J. McGaw, Investigation of the antimicrobial and anticancer activity of aminonaphthoquinones, Drug Dev. Res. 1–9 (2018), https://doi.org/10.1002/ddr.21477.
[49] D. Belorgey, D.A. Lanfranchi, E. Davioud-Charvet, 1,4-Naphthoquinones and other NADPH-dependent glutathione reductase-catalyzed redox cyclers as antimalarial agents, Curr. Pharm. Des. 19 (14) (2013) 2512–2528.
[50] A. Sendl, J.L. Chen, S.D. Jolad, C. Stoddart, E. Rozhon, M. Kernan, W. Nanakorn, M. Balick, Two new naphthoquinones with antiviral activity from Rhinacanthus nasutus, J. Nat. Prod. 59 (8) (1996) 808–811.
[51] D. Dey, R. Ray, B. Hazra, Antitubercular and antibacterial activity of quinonoid natural products against multi-drug resistant clinical isolates, Phytother. Res. 28 (7) (2014) 1014–1021.
[52] S. Shin, H. Lee, C. Jeon, U.H. Preya, J.H. Choi, J.H. Park, Anticancer activity of 2-amino-substituted-1,4-naphthoquinone derivatives in ovarian cancer cells, B Kor. Chem. Soc. 38 (12) (2017) 1411–1414.
[53] J.A. Ibacache, J. Faundes, M. Montoya, S. Mejias, J.A. Valderrama, Preparation of novel homodimers derived from cytotoxic isoquinolinequinones. A twin drug approach, Molecules 23 (2) (2018).
[54] Y.Q. Zhao, Y.H. Lu, R.D. Li, J.A. He, H. Zhang, X. Wang, Z.M. Ge, R.T. Li, Discovery and optimization of 2-thio-5-amino substituted benzoquinones as potent anticancer agents, Eur. J. Med. Chem. 149 (2018) 1–9.
[55] B.L. Liu, L.Q. Gu, J.L. Zhang, Synthesis of plastoquinone derivatives with different structures of the side-chain, Recl. Trav. Chim. Pay B 110 (4) (1991) 104–110.
[56] Y.N. Antonenko, A.V. Avetisyan, L.E. Bakeeva, B.V. Chernyak, V.A. Chertkov, L.V. Domnina, O.Y. Ivanova, D.S. Izyumov, L.S. Khailova, S.S. Klishin, G.A. Korshunova, K.G. Lyamzaev, M.S. Muntyan, O.K. Nepryakhina, A.A. Pashkovskaya, O.Y. Pletjushkina, A.V. Pustovidko, V.A. Roginsky, T.I. Rokitskaya, E.K. Ruuge, V.B. Saprunova, I.I. Severina, R.A. Simonyan, I.V. Skulachev, M.V. Skulachev, N.V. Sumbatyan, I.V. Sviryaeva, V.N. Tashlitsky, J.M. Vassiliev, M.Y. Vyssokikh, L.S. Yaguzhinsky, A.A. Zamyatnin, V.P. Skulachev, Mitochondria-targeted plastoquinone derivatives as tools to interrupt execution of the aging program. 1. Cationic plastoquinone derivatives: synthesis and in vitro studies, Biochem.-Moscow 73 (12) (2008) 1273–1287.
[57] H. Buff, U. Kucklander, Reaction of N-methyl-hydrazones as azaenamines with quinones, Tetrahedron 56 (29) (2000) 5137–5145.
[58] R.A. Tapia, C. Carrasco, S. Ojeda, C. Salas, J.A. Valderrama, A. Morello, Y. Repetto, Synthesis of indazol-4,7-dione derivatives as potential trypanocidal agents, J. Heterocycl. Chem. 39 (5) (2002) 1093–1096.
[59] C.K. Ryu, K.H. Shin, J.H. Seo, H.J. Kim, 6-Arylamino-5,8-quinazolinediones as potent inhibitors of endothelium-dependent vasorelaxation, Eur. J. Med. Chem. 37 (1) (2002) 77–82.
[60] T. Ikeda, H. Wakabayashi, M. Nakane, Preparation of benzoquinones as antiallergy and antiinflammatory agents, Pfizer Inc., USA, 1991, p. 23.
[61] P.-Y. Lu, K.-P. Chen, C.-P. Chuang, The radical reactions of imine radicals produced from the metal salts oxidation of 2-amino-1,4-benzoquinones, Tetrahedron 65 (36) (2009) 7415–7421.
[62] H. Musso, D. Doepp, I.X. Phenoxazines, Synthesis and light absorption of 8-hydroxy-3-phenoxazones, Chem. Ber. 99 (5) (1966) 1470–1478.
[63] W.A. Morgan, J.A. Hartley, G.M. Cohen, Quinone-induced DNA single-strand breaks in rat hepatocytes and human chronic myelogenous leukemic K562-cells, Biochem. Pharmacol. 44 (2) (1992) 215–221.
[64] APEX2, version 2014.1-1, Bruker, 2014, Bruker AXS Inc., Madison, WI.
[65] SAINT, version 8.34A, Bruker, 2013, Bruker AXS Inc., Madison, WI.
[66] SADABS, version 2012/2, Bruker, 2012, Bruker AXS Inc., Madison, WI.
[67] SHELXTL, version 6.14, Bruker,2000, Bruker AXS Inc., Madison, WI.
[68] A.L. Spek, Structure validation in chemical crystallography, Acta Crystallogr. D 65 (2009) 148–155.
[69] C.F. Macrae, P.R. Edgington, P. McCabe, E. Pidcock, G.P. Shields, R. Taylor, M. Towler, J. van De Streek, Mercury: visualization and analysis of crystal structures, J. Appl. Crystallogr. 39 (2006) 453–457.
[70] T.F.S. Ali, K. Iwamaru, H.I. Ciftci, R. Koga, M. Matsumoto, Y. Oba, H. Kurosaki, M. Fujita, Y. Okamoto, K. Umezawa, M. Nakao, T. Hide, K. Makino, J. Kuratsu, M. Abdel-Aziz, G.E.D.A.A. Abuo-Rahma, E.A.M. Beshr, M. Otsuka, Novel metal chelating molecules with anticancer activity. Striking effect of the imidazole substitution of the histidine-pyridine-histidine system, Bioorg. Med. Chem. 23 (17) (2015) 5476–5482.
[71] M.D. Altintop, H.I. Ciftci, M.O. Radwan, B. Sever, Z.A. Kaplancikli, T.F.S. Ali, R. Koga, M. Fujita, M. Otsuka, A. Ozdemir, Design, synthesis, and biological evaluation of novel 1,3,4-thiadiazole derivatives as potential antitumor agents against chronic myelogenous leukemia: striking effect of nitrothiazole moiety, Molecules 23 (1) (2018).

[72] H. Tateishi, K. Monde, K. Anraku, R. Koga, Y. Hayashi, H.I. Ciftci, H. DeMirci, T. Higashi, K. Motoyama, H. Arima, M. Otsuka, M. Fujita, A clue to unprecedented strategy to HIV eradication: "Lock-in and apoptosis", Sci. Rep. 7 (2017).
[73] H.I. Ciftci, H. Fujino, R. Koga, M. Yamamoto, S. Kawamura, H. Tateishi, Y. Iwatani, M. Otsuka, M. Fujita, Mutational analysis of HIV-2 Vpx shows that proline residue 109 in the poly-proline motif regulates degradation of SAMHD1, Febs Lett. 589 (13) (2015) 1505–1514.
[74] M. Karabacak, M.D. Altintop, H.I. Ccediliftci, R. Koga, M. Otsuka, M. Fujita, A. Oumlzdemir, Synthesis and evaluation of new pyrazoline derivatives as potential anticancer agents, Molecules 20 (10) (2015) 19066–19084.
[75] R. Koga, M.O. Radwan, T. Ejima, Y. Kanemaru, H. Tateishi, T.F.S. Ali, H.I. Ciftci, Y. Shibata, Y. Taguchi, J. Inoue, M. Otsuka, M. Fujita, A dithiol compound binds to the zinc finger protein TRAF6 and suppresses its ubiquitination, ChemMedChem 12 (23) (2017) 1935–1941.
[76] M.O. Radwan, S. Sonoda, T. Ejima, A. Tanaka, R. Koga, Y. Okamoto, M. Fujita, M. Otsuka, Zinc-mediated binding of a low-molecular-weight stabilizer of the host anti-viral factor apolipoprotein B mRNA-editing enzyme, catalytic polypeptide-like 3G, Bioorg. Med. Chem. 24 (18) (2016) 4398–4405.
[77] A. Tanaka, M.O. Radwan, A. Hamasaki, A. Ejima, E. Obata, R. Koga, H. Tateishi, Y. Okamoto, M. Fujita, M. Nakao, K. Umezawa, F. Tamanoi, M. Otsuka, A novel inhibitor of farnesyltransferase with a zinc site recognition moiety and a farnesyl group, Bioorg. Med. Chem. Lett. 27 (16) (2017) 3862–3866.
[78] W.E. Mehanna, T.G. Lu, B. Debnath, D.S. Lasheen, R.A.T. Serya, K.A. Abouzid, N. Neamati, Synthesis, ADMET properties, and biological evaluation of benzothiazole compounds targeting chemokine receptor 2 (CXCR2), ChemMedChem 12 (13) (2017) 1045–1054.